
Electronic Thesis and Dissertation Repository

7-21-2023 9:30 AM

Characterization of Etoxazole Resistance in *Tetranychus urticae* Populations Collected from Commercial Greenhouses & Fields in Ontario

Jeremy Spenler,

Supervisor: Grbic, Vojislava, *The University of Western Ontario*

A thesis submitted in partial fulfillment of the requirements for the Master of Science degree in Biology

© Jeremy Spenler 2023

Follow this and additional works at: <https://ir.lib.uwo.ca/etd>



Part of the [Biology Commons](#), and the [Molecular Genetics Commons](#)

Recommended Citation

Spenler, Jeremy, "Characterization of Etoxazole Resistance in *Tetranychus urticae* Populations Collected from Commercial Greenhouses & Fields in Ontario" (2023). *Electronic Thesis and Dissertation Repository*. 9642.

<https://ir.lib.uwo.ca/etd/9642>

This Dissertation/Thesis is brought to you for free and open access by Scholarship@Western. It has been accepted for inclusion in Electronic Thesis and Dissertation Repository by an authorized administrator of Scholarship@Western. For more information, please contact wlsadmin@uwo.ca.

Abstract

In this investigation, etoxazole resistance was monitored in two spotted spider mite (TSSM) populations collected from commercial greenhouses in Ontario. The frequency of an etoxazole resistant, recessive target-site mutation, I1017F, in chitin synthase I (*CHSI*) was tracked within populations over the course of the study. Cytochrome P450 (P450) activity emerged as a possible alternative mechanism to resist etoxazole exposure in one population.

Using genetic crossing between highly resistant mite populations and a susceptible lab population, filial (F1) hybrid populations were created. The recessive I1017F target-site mutation was abolished in F1 hybrids highly susceptible to etoxazole, while elevated P450 activity was not retained throughout the investigation. My data reinforces the critical role the *CHSI* I1017F mutation plays in etoxazole resistance in TSSM. Evidence for detoxification of etoxazole by P450s could not be separated from the dominant effect of the I1017F target-site mutation and further investigation into this possibility is required.

Keywords

Tetranychus urticae, etoxazole, cytochrome P450, target-site mutation.

Summary for Lay Audience

Tetranychus urticae (Koch), the two spotted spider mite (TSSM), is a widespread agricultural pest with worldwide distribution. It is an extreme generalist, capable of feeding on at least 1100 plants species, including 150 economically important crops. TSSM is very small in size with adult females, the larger of the two sexes, being 0.5 mm long. With short generation time of 7-8 days in ideal conditions and adult females being able to lay (oviposit) up to 10-13 eggs a day, a small infestation of TSSM can quickly become a serious problem for commercial growers.

Commercial growers deploy biological controls (predatory mites) and acaricides (pesticides targeting acari species) to combat mite infestations. TSSM has been shown to rapidly evolve resistance to acaricides. This can result from a change in the sequence of the gene encoding a protein that is targeted by a pesticide, referred to as a target-site mutation. Metabolic resistance can also occur when detoxifying enzymes within the mite can break down or eliminate the acaricide before it can damage the mite.

The acaricide active ingredient of etoxazole is the focus of this investigation. A recessive target-site mutation, I1017F, within the *chitin synthase I* gene has been shown to be associated with etoxazole resistance. Metabolic resistance has been implicated in a few studies, but evidence is limited. This investigation monitored the resistance status of TSSM populations over time in relation to the I1017F mutation and looked for the presence of metabolic resistance.

Acknowledgments

I would like to acknowledge my supervisor, professor Vojislava Grbic, for her support, not only during my master's program, but for giving me the opportunity to pursue a Master's degree in the first place. I would also like to thank a former technician in the Grbic lab, Biljana Popovic, for teaching me the skills and protocols to succeed in the lab. Vladimir Zhurov, the research associate in the Grbic lab, was instrumental in data analysis and as a valued resource of knowledge throughout my time in the lab. I would like to thank postdoctoral fellows Nicolas Bensoussan and Kristie Bruinsma for their help with advice in technique and experimental design. I would like to acknowledge my academic advisors, Ian Scott and Mark Bernards for their advice throughout my project. I would like to thank the past and current staff of the Biotron, Julia Nowak and Kyle Doward. Lastly, I would like to thank Hanna Varonina, a former graduate student in the Grbic lab and friend for her support throughout my time in the lab.

Table of Contents

Abstract.....	ii
Summary for Lay Audience.....	iii
Acknowledgments.....	iv
Table of Contents.....	v
List of Tables.....	viii
List of Figures.....	ix
List of Abbreviations.....	xii
1 Introduction.....	1
1.1 The two spotted spider mite, <i>Tetranychus urticae</i> Koch.....	1
1.2 Xenobiotic resistance.....	3
1.2.1 Metabolic resistance.....	3
1.2.2 Target-site mutations.....	3
1.3 Etoxazole.....	4
1.4 Chitin synthase I.....	5
1.5 Target-site mutation in <i>CHS1</i>	5
1.6 Cytochrome P450s.....	7
1.7 Thesis Objectives.....	7
Specific objectives for this investigation are:.....	7
2 Material & Methods.....	8
2.1 Plants.....	8
2.2 Mites.....	10
2.3 Pesticide.....	11
2.4 Etoxazole selection.....	11
2.5 Acaricide bioassay: ovicidal.....	12

2.6	Genotyping for I1017F	15
2.6.1	RNA extraction & isolation	15
2.6.2	cDNA synthesis	15
2.6.3	PCR & PCR purification.....	15
2.6.4	DNA sequencing reaction.....	17
2.7	Enzyme Activity Assays	17
2.7.1	Bradford assay: protein quantification.....	17
2.7.2	P450 activity assay.....	18
2.8	Genetic crossing.....	19
2.8.1	Male mite synchronization.....	19
2.8.2	Female mite synchronization	21
2.8.3	Genetic crossing: creating F1 hybrids.....	21
2.9	Survivor genotyping.....	21
2.10	Data Analysis	22
2.10.1	Quantitative sequencing.....	23
2.10.2	Dose response modelling	23
2.10.3	Genetic modelling.....	24
3	Results	25
3.1	TSSM population history	25
3.2	Etoazole selection	26
3.2.1	Etoazole resistance monitoring (Jan'20 - Jul'21)	28
3.3	P450 activity: LND, LNDE and 18E mite populations	33
3.4	Analysis of genetic crossing method	35
3.5	Genetic crossing experiment.....	39
3.5.1	Dose response: ♀LND × ♂LND	39
3.5.2	Dose response: ♀LND × ♂LNDE	40

3.5.3	Dose response: ♀LND × ♂18E	41
3.5.4	Combined dose responses plot.....	42
3.5.5	F1 hybrids deviation from expected genotype.....	44
3.5.6	P450 activity: genetically crossed populations	46
3.5.7	Genetic crossing experiment summary	48
4	Discussion	49
4.1	TSSM populations varying response to selection.....	49
4.1.1	Elevated P450 activity lost in F1 hybrids	49
4.2	Genetics of I1017F SNP buildup during etoxazole selection	50
4.2.1	Genetic models of recessive allele frequencies	51
4.3	Metabolic resistance of etoxazole.....	58
4.3.1	Scenario 1: TSSM embryo (egg) bottleneck.....	59
4.3.2	Scenario 2: Target-site mutation suppression of selection pressure	61
4.4	I1017F SNP cross resistance.....	62
5	Summary & Conclusion.....	64
6	Future directions.....	65
	References.....	67
	Appendices.....	74
	Curriculum Vitae	75

List of Tables

Table 2.1: <i>CHSI</i> primers.....	16
Table 2.2: PCR reaction mixture (1x).....	16
Table 2.3: PCR reaction cycle	16
Table 3.1: TSSM I1017F genotype shift without	25
Table 3.2: ANOVA: etoxazole mortality comparison data	28
Table 3.3: Tukey HSD table: etoxazole mortality comparison data.....	28
Table 3.4: Etoxazole selected mite populations I1017F genotype shift.	29
Table 3.5: Etoxazole selected mite populations after 19 months.....	31
Table 3.6: Etoxazole selected mite	33
Table 3.7: ANOVA: P450 activity – adults & teleios data.....	34
Table 3.8: Tukey HSD: P450 activity – adults & teleios data.....	35
Table 3.9: LND male crossing theoretical outcome.	36
Table 3.10: LND female crossing theoretical outcome.	36
Table 3.11: Ratio of males in genetic crossing experiment water controls	39
Table 3.12: Survivor genotype.....	45
Table 3.13: ANOVA: P450 activity – genetic crossing experiment data.	47
Table 3.14: Tukey HSD: P450 activity – genetic crossing experiment data	48
Table A1: Software Information.	74

List of Figures

Figure 1.1: <i>Tetranychus urticae</i> life cycle	2
Figure 1.2: TSSM colony on red kidney beans.....	2
Figure 1.3: Etoxazole structure model	4
Figure 1.4: Chitin synthase I.....	6
Figure 1.5: Etoxazole hypothetical mode of action	6
Figure 2.1: Bean plant production (Pre-July 2022)	9
Figure 2.2: Bean plant production (post July 2022)	10
Figure 2.3: TSSM lab colony setup	11
Figure 2.4: Ovicidal experimental setup.....	13
Figure 2.5: Ovicidal experiment incubation	14
Figure 2.6: 1020 tray setup	20
Figure 2.7: Female & male synchronization timeline to create genetic crosses	20
Figure 2.8: Survivor transfer to leaf.....	22
Figure 3.1: Etoxazole mite population history.....	26
Figure 3.2: Etoxazole mortality comparison.....	27
Figure 3.3: Dose response curves – etoxazole selection (11 months)	30
Figure 3.4: Dose response curves – etoxazole selection (11 & 19 months)	31
Figure 3.5: Dose response - LNDE & 18E (Feb-Mar, 2022).....	32
Figure 3.6: P450 activity – adults & teleios.....	34

Figure 3.7: Genetic crossing methods.....	36
Figure 3.8: Dose response curves – genetic crossing pilot (σ LND)	37
Figure 3.9: Dose response curves – genetic crossing pilot (ϕ LND)	38
Figure 3.10: Dose response curve - ϕ LND \times σ LND.....	40
Figure 3.11: Dose response curve - ϕ LND \times σ LNDE	41
Figure 3.12: Dose response curve - ϕ LND \times σ 18E.....	42
Figure 3.13: Dose response curve – genetic crossing experiment	43
Figure 3.14: P450 activity – genetic crossing experiment.....	47
Figure 4.1: I1017F SNP frequency, 11 to 31 months	51
Figure 4.2: Recessive allele frequency model	52
Figure 4.3: Genetic drift recessive allele frequency models.....	54
Figure 4.4: Inbreeding effects on heterozygosity	55
Figure 4.5: Genotype frequency vs recessive allele frequency.....	56
Figure 4.6: Haplodiploid allele fixation.....	57
Figure 4.7: Gene expression heatmaps by development stage	60
Figure 4.8: Target-site suppression of selection pressure model.....	62

List of Appendices

Appendix A: Software used during investigation.....	74
---	----

List of Abbreviations

7-EFC	7-ethoxy-4-trifluoromethylcoumarin
7-HFC	7-hydroxy-4-trifluoromethylcoumarin
ABC	ATP-binding cassette transporter
BSA	bovine serum albumin
CCE	carboxyl/cholinesterases
cDNA	complementary deoxyribonucleic acid
CHS1	chitin synthase I protein
<i>CHS1</i>	chitin synthase 1 gene
ddAH ₂ O	double distilled then autoclaved water
DNA	deoxyribonucleic acid
F1	Filial 1
GABA	gamma-aminobutyric acid
GlcNAc	<i>N</i> -acetylglucosamine
GST	glutathione-S-transferase
I1017F	phenylalanine substitution for isoleucine at position
LC 90	lethal concentration 90%
LND	<i>Tetranychus urticae</i> – London colony
LNDE	etoxazole selected London colony mite
NADP ⁺	nicotinamide adenine dinucleotide phosphate
NADPH	reduced form of NADP ⁺
P450	cytochrome P450
PCR	polymerase chain reaction
pH	potential of hydrogen
RH	relative humidity

RNA	ribonucleic acid
RR	resistance ratio
SNP	single nucleotide polymorphism
TSSM	two spotted spider mite
$\mu\text{mol m}^{-2} \text{s}^{-1}$	μmol of photons per second and square meter
##E	numbered etoxazole selected mite population

1 Introduction

1.1 The two spotted spider mite, *Tetranychus urticae* Koch

Tetranychus urticae is a polyphagous, herbivorous arthropod of the Acari subclass of Arachnida, belonging to the Tetranychidae family. Commonly called the two spotted spider mite (TSSM), it is an extreme generalist, capable of feeding on more than 1,100 plant species (Migeon & Dorkeld, 2006-2023). TSSM reproduce through arrhenotokous parthenogenesis, with unfertilized eggs developing into haploid males and fertilized eggs developing into diploid females (Oliver, 1971; Hebert, 1981). The TSSM life cycle is composed of five stages: egg, larvae, two nymph stages (proto-nymph then deuto-nymph) and the final adult stage, with a quiescent chrysalis phase between mobile stages (Figure 1.1) (Liburd & Finn, 2004). During the chrysalis phase the TSSM grows in size and undergoes the molting process, forming a new, larger exoskeleton and discarding their old one as they progress towards adulthood (Zhao et al., 2017). TSSM use a stylet to feed on the cellular contents of mesophyll cells, resulting in cellular death and formation of chlorotic spots on plant leaves (Figure 1.2 A & B and Bensoussan et al., 2016). Mite maturation is dependent on environmental conditions. TSSM favor warmer temperatures, taking nine days to develop from oviposition of an egg to adult at 26°C with 40% RH (Liburd & Finn, 2004). Adult TSSM are 0.4 - 0.5 mm in length and typically are light green in appearance with two dark spots (Liburd & Finn, 2004).

The TSSM is a major pest in agriculture, feeding on more than 150 crops in both field and greenhouse settings, including cucumbers, peppers, strawberries, soy, tomatoes, apples, and grapes (Migeon & Dorkeld, 2006-2023). The TSSM is distributed in over 5380 geographical locations in 124 countries, making it a worldwide agricultural pest (Tuan et al., 2016; Migeon & Dorkeld, 2006-2023). The natural characteristics of the TSSM such as small size, short generation time, high fecundity, and arrhenotokous parthenogenesis help the TSSM to rapidly develop resistance to pesticides (Van Leeuwen et al., 2009). TSSM is becoming the most pesticide resistant pest in the world, with resistance to 93 active ingredients being recorded (Sparks & Nauen, 2015). Analysis of the genome of the

TSSM has revealed expansions in gene families involved in the digestion, detoxification, and transport of xenobiotics when compared to insects (Grbic et al., 2011).

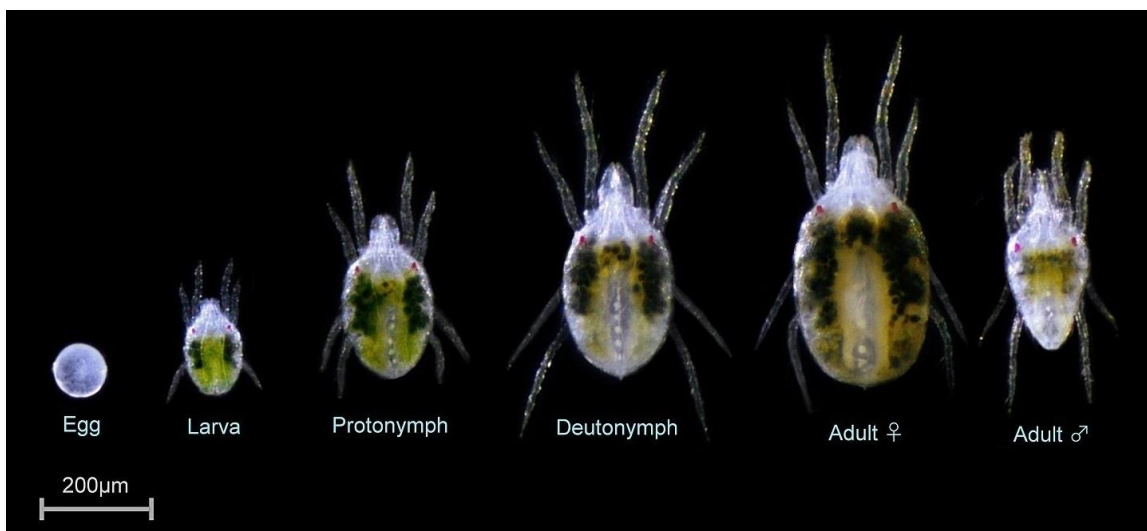


Figure 1.1: *Tetranychus urticae* life cycle. TSSM life cycle stages and sexual dimorphic adults. Chrysalis stages between mobile ones are not shown. (Images courtesy of Zoran Culo).

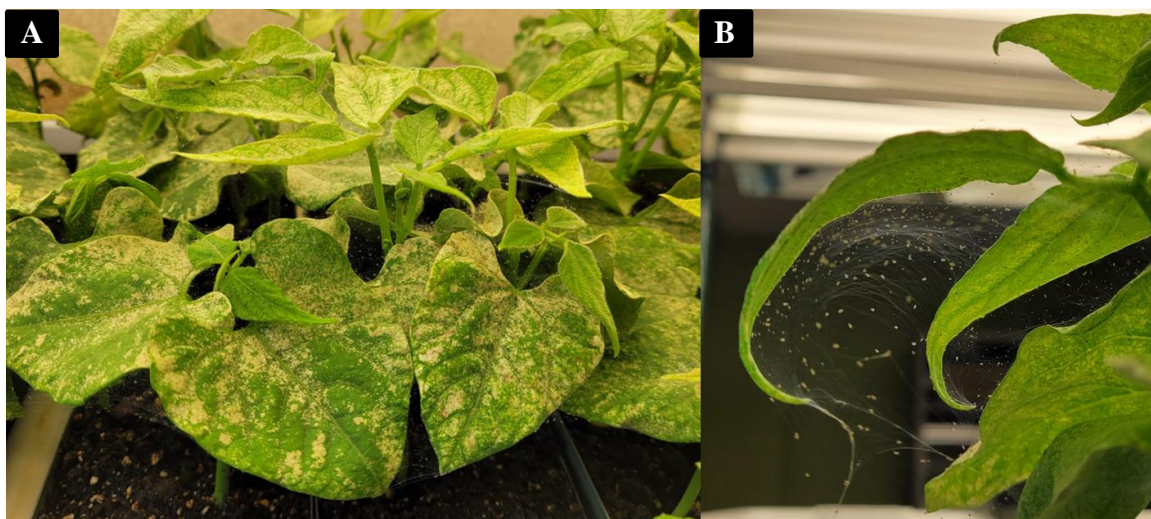


Figure 1.2: TSSM colony on red kidney beans. A) A TSSM colony on red kidney bean plants exhibiting chlorotic damage caused by mite feeding on mesophyll cells. B) Silk deposited on infested plants by a TSSM colony. (Images courtesy of Zoran Culo).

1.2 Xenobiotic resistance

Adaptations by organisms to overcome the effects of toxic xenobiotic compounds are usually broken down into pharmacokinetic and pharmacodynamic mechanisms (Van Leeuwen & Dermauw, 2016). Pharmacokinetic mechanisms involve those that result in decreased exposure to a xenobiotic, including increased metabolism and behavioral changes to avoid the xenobiotic (Van Leeuwen & Dermauw, 2016). Pharmacodynamic mechanisms refer to those that cause decreased sensitivity to the xenobiotic, such as target-site mutations (Van Leeuwen & Dermauw, 2016). Resistance due to increased metabolism of xenobiotics and target-site mutations was the focus of this investigation.

1.2.1 Metabolic resistance

Metabolism of xenobiotics takes place in three phases, in phase I; the xenobiotic has functional groups added to make it more water-soluble and reactive, in phase II; xenobiotics are conjugated to endogenous metabolites, and in phase III; the conjugated xenobiotics are excreted (Kennedy & Tierney, 2013). TSSM have expanded gene families encoding glutathione-S-transferases (GSTs), cytochrome P450 (P450s), ATP-binding cassette transporters (ABCs), and carboxyl/cholinesterases (CCEs) when compared to insects (Grbic et al., 2011). Mutations associated with these genes, causing upregulation of detoxifying enzymes, by duplication, amplification, and changes in cis and trans regulatory elements, can further augment the TSSM's ability to develop resistance (Feyereisen et al., 2015).

1.2.2 Target-site mutations

Active ingredients of acaricides bind and affect the function of the endogenous mite proteins. Targets of effective acaricides are proteins essential for mite development and survival, thus, acaricide application ultimately leads to mites' death. Pesticides have specific target-sites that they interact with to exert their toxic effects. Mutation in the gene encoding a target protein that preserves the target protein function in the presence of the pesticide leads to the target-site resistance. It can result from the increased expression of the target gene or a change in the structure of the gene product that prevents the interaction between the pesticide and the target protein (Van Leeuwen & Dermauw, 2016).

Historically, in TSSM there were three main target-site mutations known to lead to resistance to specific classes of pesticides (Van Leeuwen & Dermauw, 2016). For example, mutation in acetylcholinesterase can lead to resistance to organophosphates, voltage-gated sodium channel mutations can lead to resistance to pyrethroids and dicofol, and mutations in GABA-gated chloride channels can lead to resistance in organochlorines and phenylpyrazoles (Van Leeuwen & Dermauw, 2016).

1.3 Etoxazole

Etoxazole was developed in Japan and was first synthesized by Ishida et al. in 1994. It was commercialized in 1998 by Yashima Chemical Industries (Merzendorfer, 2013). Etoxazole is an organofluorine insecticide with the chemical name of 2-(2,6-difluorophenyl)-4-[4-(1,1-dimethylethyl)-2-ethoxyphenyl]-4,5-dihydrooxazole (Figure 1.3) (Dekeyser, 2005).

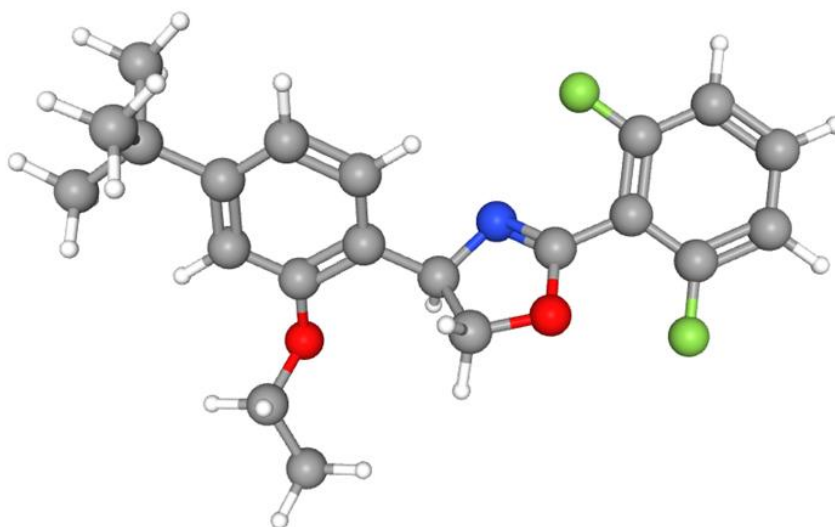


Figure 1.3: Etoxazole structure model. $C_{21}H_{23}F_2NO_2$, Carbon (grey) and hydrogen (white) form the majority of the structure, with fluorine (green), nitrogen (blue), and oxygen (red) atoms (National Center for Biotechnology Information, 2021).

Etoxazole was shown to be effective at causing mortality in mite eggs, larvae, and nymphs while reducing the fertility of adult females (Dekeyser, 2005; Van Leeuwen et al., 2012). More recently, etoxazole has been shown to inhibit mite growth by interfering with the

activity of chitin synthase I (CHS1) (Van Leeuwen et al., 2012). Etoxazole also exhibits toxicity towards non-mite arthropods and aquatic invertebrates (Arena et al., 2017).

1.4 Chitin synthase I

Chitin is an amino polysaccharide that is a key component providing mechanical strength to the exoskeletons of arthropods, including TSSM (Merzendorfer, 2006). Chitin is composed of linear polymers of β -(1-4)-linked N-acetyl-glucosamines (GlcNAc) assembled into larger microfibrils (Merzendorfer, 2006). Chitin synthases, a family of glycosyltransferases, form the glycosidic bonds between GlcNAc units (Merzendorfer, 2006). CHS1 is a transmembrane protein with the catalytic active site located in the cytoplasm of the cell (Figure 1.4 and Merzendorfer, 2006; Merzendorfer, 2013). CHS1 has five transmembrane domains forming a translocation pore for the transportation of newly formed chitin chains to the extracellular space (Merzendorfer, 2013). These pores are formed by the trimeric complex of individual CHS1 proteins (Merzendorfer, 2013).

1.5 Target-site mutation in *CHS1*

A fully recessive target-site mutation in a transmembrane domain of *CHS1*, I1017F, has shown a strong correlation to etoxazole resistance in TSSM (Van Leeuwen et al., 2012; Van Leeuwen & Dermauw, 2016). The mutation (I1017F) is in one of the transmembrane protein domains that form the translocation pore (Merzendorfer, 2013). The mode of action of etoxazole is not known, however, two possible methods have been hypothesized. According to the first possibility, the binding of etoxazole blocks the translocation pore in CHS1 (Figure 1.5 B). Alternatively, the misalignment of chitin chains during translocation inhibits fibrillogenesis (Figure 1.5 C) (Merzendorfer, 2013). Fibrillogenesis is the formation of microfibrils from the individual chitin chains, a process that is proposed to be sensitive to proper orientation of chitin chains (Merzendorfer, 2013).

Chitin synthase I

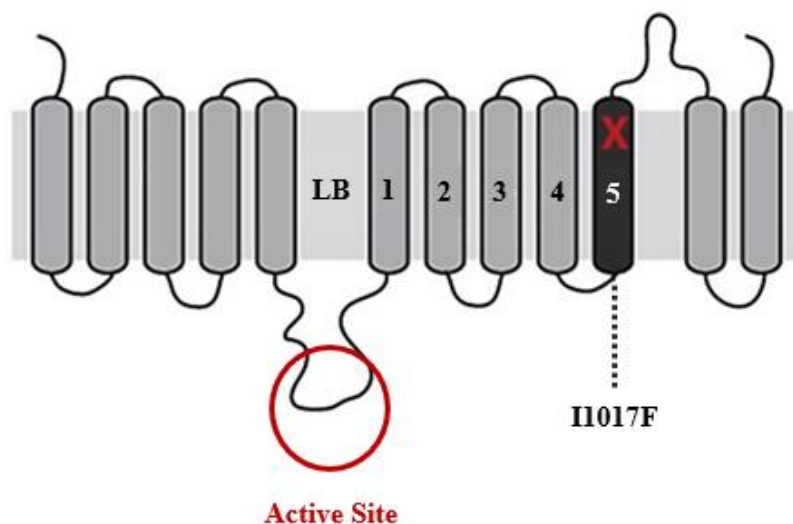


Figure 1.4: Chitin synthase I. A schematic of the protein domains of the chitin synthase I (CHS1) protein. Domains labelled 1 through 5 form a pore in the lipid bilayer of a cell, allowing chitin chains to exit the cell (Demaeght et al., 2014).

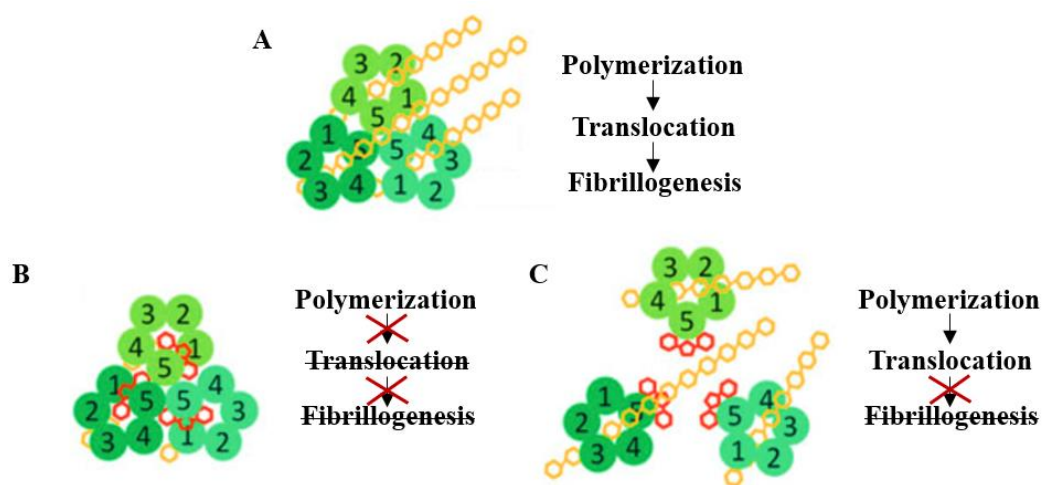


Figure 1.5: Etoxazole hypothetical mode of action. (A) The functional arrangement of protein domains (labelled 1–5) forming a translocation pore, (B) etoxazole binding within the pore blocks the translocation of chitin chains, and (C) etoxazole binding disrupts the trimeric CHS1 complex, resulting in chitin chain translocation that lacks proper orientation for fibrillogenesis (Merzendorfer, 2013).

1.6 Cytochrome P450s

Cytochrome P450s are a family of enzymes that catalyze oxidation reactions typically resulting in the addition of an OH- group to a wide range of substrates, including both xenobiotics and endogenous compounds (Feyereisen, 2005, 2006). P450s were shown to play a major role in metabolic resistance to pesticides in many agricultural pests, including the TSSM (Feyereisen, 2005, 2006). The genome of the TSSM has 86 genes encoding P450 enzymes (Grbic et al., 2011). The overexpression of P450s was associated with resistance to acaricides. For example, mite resistance to abamectin was associated with increased expression of several P450s (Dermauw et al., 2013). Though limited, a 2017 study (Adesanya et al., 2017) implicated P450s and esterases (CCEs) as possible contributing factors to etoxazole resistance in TSSM. Another study identified P450s, CCEs, and GSTs in the resistance to etoxazole of the predatory mite, *Phytoseiulus persimilis* (Salman et al., 2015).

1.7 Thesis Objectives

The TSSM has a well-characterized association between mite resistance to etoxazole and the I1017F substitution in the *CHSI* gene. The *CHSI* I1017F substitution confers a high level of etoxazole resistance to mites that are homozygous for the resistant allele. Evidence for the metabolic resistance to etoxazole in TSSM is scarce by comparison. If metabolic resistance to etoxazole is present in TSSM, it will also have implications on mite cross-resistance to other pesticides, buildup of the I1017F allele, and the pest control strategies in situations where etoxazole is deployed.

Specific objectives for this investigation are:

- A) To test if the target-site mutation (I1017F SNP) is predictive of the etoxazole resistance status in Ontario TSSM field populations;
- B) To test if detoxifying enzymes contribute to etoxazole resistance in Ontario TSSM field populations.

2 Material & Methods

As a foreword to this section, this investigation encountered difficulties related to the Covid-19 pandemic. This mainly pertained to TSSM sample acquisition from commercial growers. However, this also caused changes in the overall design of the investigation and timelines of experiments, as the investigation had to shift to the use of TSSM samples already on hand in the lab.

2.1 Plants

The plants used in this investigation were *Phaseolus vulgaris*, California Red Kidney Beans (Stokes Seed Ltd., Thorold, Ontario, Canada) and later Dark Red Kidney Beans (Gentec Inc., Twin Falls, Idaho, USA), grown on a sphagnum peat moss based growing mix, Pro-Mix BX mycorrhizae (Plant Products Inc., Leamington, Ontario, Canada). There were two phases of growth conditions (Pre-July 2022, and Post-July 2022). This was due to a transition to a new growth chamber in the Biotron Institute for Experimental Climate Change Research (Biotron), Western University. Pre-July 2022 growth chamber conditions were $26 \pm 2^\circ\text{C}$ with a relative humidity (RH) of 60% on a 16:8-hour (light: dark) photoperiod with a cool-white, fluorescent light setup (Philips, very high output F96T12/CW/VHO/EW) at a light intensity of 120-150 micromole per second and meter squared ($\mu\text{mol m}^{-2} \text{s}^{-1}$) (Figure 2.1). Post-July 2022 growth chamber conditions were $26 \pm 2^\circ\text{C}$ with a RH of 60% on a 16:8-hour (light: dark) photoperiod with red wavelength boosted light (Philips GreenPower LED Production Module 3.0 Dynamic GPL PM 168 DRBWFR L120 G3.0 C4 NA) at 120-150 $\mu\text{mol m}^{-2} \text{s}^{-1}$ (Figure 2.2). The change in conditions was due to upgrades in the growth chambers, allowing for additional lighting parameters. Kidney beans grown in the red wavelength boosted light had shorter stems and the leaves were slightly enlarged. Fecundity of a London lab TSSM mite population (LND) was assessed on plants from both chambers and found to be similar.



Figure 2.1: Bean plant production (Pre-July 2022). Red kidney beans in a Biotron growth chamber, $26 \pm 2^\circ\text{C}$ with a RH of 60% on a 16:8-hour (light: dark) photoperiod with a cool-white, fluorescent light.



Figure 2.2: Bean plant production (post July 2022). Red kidney beans in a Biotron growth chamber, $26 \pm 2^\circ\text{C}$ with a RH of 60% on a 16:8-hour (light: dark) photoperiod with a red wavelength boosted light.

2.2 Mites

Mite populations used for this investigation were originally collected in the fall of 2018 from commercial greenhouses in southern Ontario. The 18 greenhouse populations were collected from various host plants, mostly tomato, but also cucumber, pepper, and eggplant. After collection, mite populations were used to start individual colonies that could be maintained in the lab for further analysis. These colonies were maintained on stem cut bean plants in an 8.4 L (32 cm x 22.8 cm x 16.4 cm) rectangular plastic container with a vented lid. Plants were supported by a plastic grid (Figure 2.3). Mite colonies were stored in a growth chamber at 25°C on a 16:8-hour (light: dark) photoperiod with a cool-white,

fluorescent light at a light intensity of $80\text{-}120 \mu\text{mol m}^{-2} \text{s}^{-1}$. This setup allowed long-term maintenance of mite colonies, provided fresh bean plants were added at regular intervals.

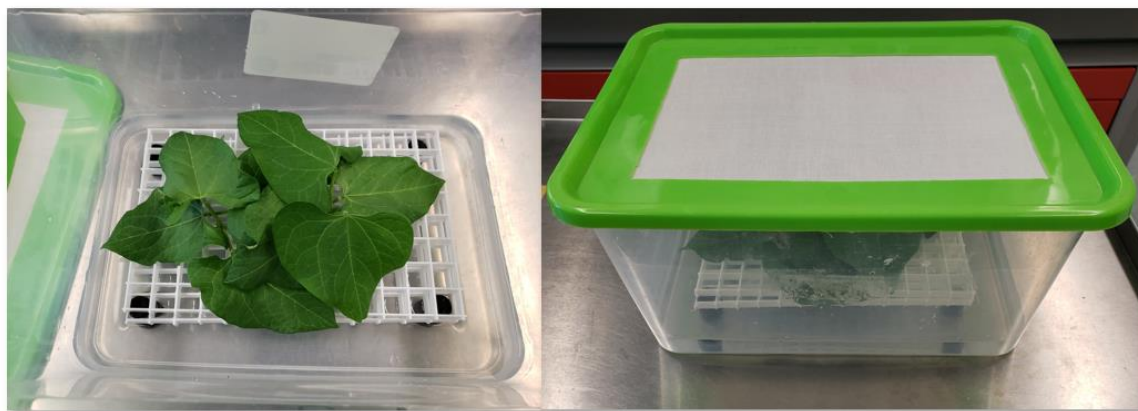


Figure 2.3: TSSM lab colony setup. Stem cut bean plants in an 8.4 L (32 cm x 22.8 cm x 16.4 cm) plastic container on a white plastic grid support with a water barrier to provide water to the plants and prevent mite escape, covered with a vented lid.

2.3 Pesticide

TetraSan™ 5 WDG Miticide, containing 5% of the active ingredient etoxazole, was used in this investigation. A product of Valent Canada Inc. (Guelph, ON, Canada), it was provided by Ian Scott, AAFC, London, ON. Tetrasan comes in pellet form and is mixed with water with continuous agitation and applied at field rates of 600 – 1200 mg/L (ppm), with an active ingredient concentration of etoxazole at 30 – 60 mg/L (Valent, 2015).

2.4 Etoxazole selection

A subset of the original 18 greenhouse collected TSSM populations was chosen for etoxazole selection. For that, the bean plants used for mite maintenance were treated by dipping the entire stem cut plant in etoxazole for 5 seconds. The etoxazole concentration used for treatment was 0.02 mg/L (ppm), an approximation of the LC90 of the susceptible LND spider mite population (LC = 0.0196 mg/L, Dec. 2019).

2.5 Acaricide bioassay: ovicidal

The ovicidal bioassay experimental setup used a 60 × 15 mm polystyrene culture dish base (60 × 15 mm Easy Grip Tissue Culture Dish, Corning™ Falcon™), 15 ml of 0.8% agar medium (Fisher Scientific), and a polystyrene cover with a 2 cm diameter circular opening, covered by nylon mesh (100µm openings, Sefar Nytel PA-13 XXX-100, Sefar BDH). Four bean leaf disks (1.5 cm in diameter) with adaxial face up were placed on top of the agar (Figure 2.4). On day 0 of a trial, each leaf disk was infested with 5 adult female mites, using a fine brush (Princeton Select Short Liner Brush, 18/0), then sealed with Parafilm (Bemis™ Parafilm™ M Laboratory Wrapping Film). After 24 hours the adult mites were removed by vacuum pump, leaving 20 – 70 eggs per leaf disk. The leaf disks were dipped into etoxazole solutions using forceps for 5 seconds, with H₂O (double distilled, ddH₂O) serving as a negative control. Mortality, considered to be the failure of an egg to hatch, was assessed on days 5 and 9 (endpoint of a trial), a healthy egg typically hatches in 4.5-5 days when kept in the ovicidal bioassay incubation conditions. The majority of mites (>95%) could be assessed on day 5. Counts on day 9 served to ensure all survivors were assessed. A mite was counted as alive if hatching occurred. Unhatched eggs were counted as dead. The experiment was performed at 26 ± 2°C, 40% RH, 20 – 50 µmol m⁻² s⁻¹ on a 16:8-hour (light: dark) photoperiod (Figure 2.5). The bioassay was performed with 20 adult mites/replica, resulting in 80-200 eggs per replica. The experiment was performed in 3 independent trials. Ovicidal bioassay data was used to construct dose response curves for sampled TSSM populations, see details in section 2.10.2.



Figure 2.4: Ovicidal experimental setup. 60 × 15 mm Easy Grip Tissue Culture Dish with 0.8 % agar to support 1.5 cm diameter leaf disks. Capable of supporting leaf disks for approximately 12 days.



Figure 2.5: Ovidal experiment incubation. Ovidal experiment setups stored in a controlled chamber at $26 \pm 2^\circ\text{C}$, 40% RH, $20 - 50 \mu\text{mol m}^{-2} \text{s}^{-1}$ on a 16:8-hour (light: dark) photoperiod.

2.6 Genotyping for I1017F

2.6.1 RNA extraction & isolation

For RNA extraction 50-100 adult female mites (unless otherwise specified) were collected by vacuum pump into a microcentrifuge tube and were immediately frozen in liquid nitrogen. The samples were processed using the RNeasy Mini Kit (Qiagen) following the manufacturer's instructions. The protocol was aided by the use of a pellet pestle mixer (Pellet Pestle Motor, Kontes) and polypropylene pellet pestles. The RNA was resuspended in 20 - 40 μ L of RNase free water (depending on volume of material collected), then quantified on a NanoDrop 2000C Spectrophotometer (Thermo Scientific).

2.6.2 cDNA synthesis

RNA isolated from mite strains was used as a template for cDNA synthesis using Maxima First Strand cDNA Synthesis Kit (Thermo Scientific). Samples of 600 ng RNA were used in a reaction following the manufacturer's protocol, and incubation steps were done in a T100 Thermal Cycler (Bio-Rad).

2.6.3 PCR & PCR purification

CHSI PCR primers were reported in Van Leeuwen et al., 2012 (Table 2.1). These primers were used in a polymerase chain reaction (PCR) to amplify a 542 bp DNA fragment containing the I1017F SNP. The 25 μ L PCR reaction (Table 2.2) and reaction conditions (Table 2.3) were carried out on a T100 Thermal Cycler (Bio-Rad). Agarose gel electrophoreses (0.8% gel) was used to confirm the presence and size of the PCR fragments. DNA bands in the gel were imaged on a ChemiDoctm Imaging System (Bio-Rad) using a 5 μ L aliquot of each reaction.

Table 2.1: CHS1 primers.

ID	Primer	Annealing temperature (°C)	Product size (bp)
TuCHS1_diaF	TGTCCGCTTGTATGCACTACT	60	542
TuCHS1_diaR	GCCACCAAGTGGGTCAAGAT	62	

Table 2.2: PCR reaction mixture (1x)

Component	Volume (μL)
ddAH ₂ O	17.35
10x Reaction buffer	2.50
25 mM MgCl	2.50
10 mM dNTPs	0.5
10 μM primer mix	1.0
cDNA template	1.0
Taq polymerase	0.15
Total	25

Table 2.3: PCR reaction cycle

Step - Temperature	Time
1. 95°C	3 min
2. 95°C	15 s 30 s 45 s
55°C	
72°C	
3. 72°C	3 min

The PCR product was purified using a manual ethanol precipitation protocol. The 20 μL of PCR product (remaining after checking 5 μL on gel) were mixed with 2 μL sodium acetate, 1.2 μL glycogen, and 40 μL ethanol (100%). The mixture was cooled at -20°C for a minimum of 30 minutes. The samples were then centrifuged (10,000 rpm) and decanted, washed with ethanol (70%), centrifuged (10,000 rpm) and decanted, and air dried before being resuspended in 20 μL of water (ddAH₂O). The purified PCR product was quantified on a NanoDrop 2000C Spectrophotometer (Thermo Scientific).

2.6.4 DNA sequencing reaction

DNA sequencing was done by Robarts Research Institute (Schulich School of Medicine & Dentistry, Western University). Reactions were set up as per Robarts instructions, 10 μL of 20 $\text{ng}/\mu\text{L}$ DNA template per reaction with 5 μL of 2 μM primer added to each tube. DNA sequence data provided by Robarts was used to determine the frequency of the *CHSI* I1017F SNP of the TSSM samples, see details in section 2.10.1.

2.7 Enzyme Activity Assays

Efforts to perform enzymatic assays on eggs were undertaken, as this was the stage of development the ovicidal bioassays were performed on. Unfortunately, the collection of eggs in quantities high enough to perform enzymatic activity assays on were not successful. Mite eggs would adhere to any surface used (plastic, glass, metal) regardless of any attempts to coat these surfaces to reduce adherence of eggs or the use of laboratory detergents. During this investigation, enzyme activity assays performed on female adult mites or teleiochrysalises (teleios), the chrysalis phase between deutonymph and adult, as indicated.

2.7.1 Bradford assay: protein quantification

To quantify the protein concentration in the collected mite samples I used the Bradford assay. The Bradford assay uses the dye Coomassie Brilliant Blue G-250 that converts from red to blue upon protein binding, causing a shift in maximum wavelength of absorption from 465 nm to 595 nm (Bradford, 1976). The Bradford assay in this investigation was done using the Quick Start™ Bradford 1x Dye Reagent (BioRad). Collected mite samples were homogenized with a pellet pestle mixer in 175 - 350 μL (depending on volume of mites in sample) of cold 0.1 M sodium phosphate buffer (pH 7.5). The homogenized samples were centrifuged at 10,000 rpm for 10 minutes at 4°C and the supernatant was transferred to new microcentrifuge tubes for use in a Bradford assay. Standards were made using bovine serum albumin (BSA) at 100, 200, 400, 600, 800, and 1000 $\mu\text{g}/\text{mL}$ of protein in sodium phosphate buffer. The standards, a blank of sodium phosphate buffer, and the samples for analysis were pipetted into a 96-well plate (Thermo Scientific™ Nunc microwell 96-well optical-bottom™ plates with polymer base, clear), with

3 technical replicas of 5 μL volumes. 250 μL of Bradford reagent was added to each well, mixed, and the reaction was allowed to proceed in the dark for 30 minutes. The plate was transferred for reading to a SpectraMax M2 (Molecular Devices), absorption of light at 595 nm was read for each well, allowing for construction of a standard curve and quantification of the concentration of protein for each sample plated.

2.7.2 P450 activity assay

Following quantification with the Bradford assay, dilutions of each sample were made to a protein concentration of 200 $\mu\text{g}/\text{mL}$ for use in a P450 activity assay. The activity of P450 is quantified by the O-deethylation of 7-ethoxy-4-trifluoromethylcoumarin (7-EFC) by P450 enzymes to the fluorescent 7-hydroxy-4-trifluoromethylcoumarin (7-HFC) molecule (Stumpf & Nauen, 2001). 7-HFC fluoresces at wavelength of 510 nm and is excited at a wavelength of 410 nm using a spectrophotometer (Stumpf & Nauen, 2001). A reaction mixture of 0.4 mM 7-EFC, 0.2 mM NADP^+ , 1 mM glucose-6-phosphate, and 0.014 U/reaction of glucose-6-phosphate dehydrogenase in 0.1 M sodium phosphate buffer pH 7.4 was made for the assay. P450 activity requires the NADPH-dependent cytochrome P450 reductase (CPR), however NADPH is fluorescent and may interfere with the accuracy of the assay (Feyereisen, 2005; Stumpf & Nauen, 2001). The reaction mixture provides NADPH as needed by reducing NADP^+ by action of glucose-6-phosphate dehydrogenase on glucose-6-phosphate, without producing excess NADPH. An opaque 96-well plate (Thermo Scientific™ Nunc microwell 96-well optical-bottom plates with polymer base, black) was used for the assay. 50 μL of mite protein extract samples was used per well and buffer blanks (0.1 M sodium phosphate pH 7.4 and 7.5) were added with 3 technical replicas. The 96-well plate remained on ice during the additions. A volume of 50 μL of the reaction mixture was added to each well containing samples or blanks. The 96-well plate was then covered with aluminum foil, as the reaction is light sensitive. The 96-well plate was removed from ice and incubated at 37°C for 30 minutes at 200 rpm in (New Brunswick Innova 4300 Incubator Shaker). The reaction with Bradford reagent was stopped after 30 minutes by adding 100 μL of a 1:1 mixture of acetonitrile and 0.05 M trizma base buffer pH 10.0 to each well, stopping the production of 7-HFC and NADPH. 100 μL of 7-HFC standards ranging in concentration from 200–2000 μM were then added into empty wells

of the 96-well plate with 3 technical replicas. Fluorescence was read on a SpectraMax M2 spectrophotometer with an excitation wavelength of 410 nm and an emission wavelength of 510 nm. A standard curve was constructed from the data to determine the concentration of 7-HFC produced by the mite protein extract samples during the assay.

2.8 Genetic crossing

Genetic crosses were created between mite populations with high etoxazole resistance (LNDE, 18E) and a susceptible lab population (LND). Females were from the LND population with no detectable frequency of the I1017F SNP. At the time of the genetic crossing, the etoxazole resistant populations LNDE and 18E had an I1017F SNP frequency of 100%. The fundamental reason for the genetic crossing was to create offspring that would be heterozygous for the recessive I1017F SNP. As such, the progeny would lose the genetic component of etoxazole resistance. The protocol for making the genetically crossed mites involves 3 separate steps: synchronizing a population of male mites, synchronizing a population of female mites, and finally coupling these synchronized mites to produce hybrid offspring.

2.8.1 Male mite synchronization

Synchronization of male mite populations started with collecting female teleios. These teleios are transferred by vacuum pump onto cut bean leaves that have been surrounded by cotton and placed in a 1020 plastic tray, supported by a plastic grid and covered by a vented lid (Figure 2.6). A total of 50 – 60 teleios are deposited on each leaf, all from the same population. The trays were incubated at $26 \pm 2^\circ\text{C}$, 40% RH, $80 - 100 \mu\text{mol m}^{-2} \text{s}^{-1}$ on a 16:8-hour (light: dark) photoperiod for 3 days. During this time, the virgin adult females emerged from the teleiochrysalises, fed, and oviposited unfertilized eggs. After 3 days, females were removed by vacuum pump, leaving the unfertilized eggs to develop into only male progeny after another 7 days of incubation. The total male synchronization method takes 10 days (Figure 2.7).

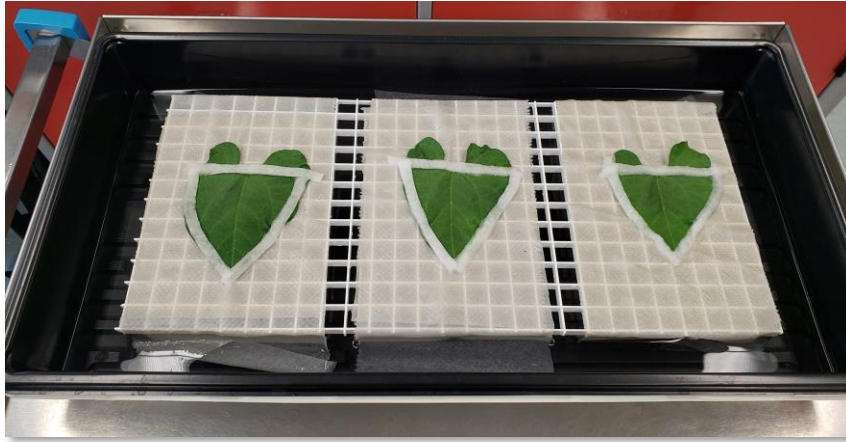


Figure 2.6: 1020 tray setup. Plastic 1020 tray with white plastic grid that supports cut bean leaves isolated by cotton, covered by a vented lid (not pictured) when incubated.

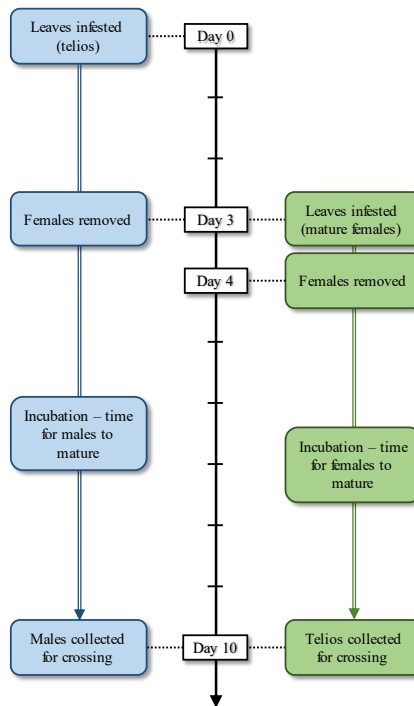


Figure 2.7: Female & male synchronization timeline to create genetic crosses. Schematic of the workflow and timing on female and male synchronization to allow for same day sampling for genetic crossing experiment.

2.8.2 Female mite synchronization

Preparation of a synchronized female population used the same setup (1020 tray and cut leaves) and incubation conditions; however, the leaves were infested with 120 mature female mites taken from the general population of the LND mite strain. After 24 hours, the female mites were removed by vacuum pump. The deposited eggs yielded both male and female offspring, with the majority being female. The eggs were incubated for a further 6.5 days until the majority were in a teleiochrysalis stage for collection. The female synchronization protocol takes ~7.5 days.

2.8.3 Genetic crossing: creating F1 hybrids

After synchronization of both sexes, a 1020 tray with cut bean leaves, isolated by cotton, with vented lid was again used as an isolated arena for male and female coupling (Figure 2.6). Teleios from the synchronized female leaves were transferred by vacuum pump, a total of 100–120 per leaf. Adult males from the male synchronization leaves were transferred by vacuum pump to the leaves with female teleios so that they outnumbered the females by a 2:1–3:1 ratio, depending on male mite availability. The leaves were incubated at $26 \pm 2^\circ\text{C}$, 40% RH, $80\text{--}100 \mu\text{mol m}^{-2} \text{s}^{-1}$ on a 16:8-hour (light: dark) photoperiod for 48 hours. The 48-hour incubation allowed for adult female to emerge from their chrysalis, feed, and allow fertilization by males. The female mites were then ready to be used for ovicidal bioassays to determine the etoxazole resistance status of the F1 progeny of genetically crossed mite populations.

2.9 Survivor genotyping

In order to determine the genotype of TSSM that survived etoxazole treatment, the ovicidal bioassay described in 2.5, was modified. After the day 5 mortality assessment the leaf disks were removed from the ovicidal setups and placed inverted on a stem cut leaves. The leaves were isolated by cotton in a 1020 plastic tray incubated at $26 \pm 2^\circ\text{C}$, 40% RH, $20 - 50 \mu\text{mol m}^{-2} \text{s}^{-1}$ on a 16:8-hour (light: dark) photoperiod (Figure 2.8). The inverted leaf disks allowed surviving larvae and nymphs to move to the whole leaf. The leaves provided food for the additional time to allow the mites to mature into adults, 4 – 5 days. After the mites matured, they were collected by vacuum pump for genotyping. Males and

female mites were collected separately. Etoxazole treatments were done in triplicate per concentration per population and survivors pooled with all survivors collected. The etoxazole concentrations of 0.02 mg/L, 0.055 mg/L, and 10 mg/L were used with LND and F1 hybrids mites. Genotyping was done as described in (2.10.1).



Figure 2.8: Survivor transfer to leaf. Leaf disks inverted on a cut bean leaf isolated by cotton, allowing immature TSSM to transfer from the disks onto the leaf.

2.10 Data Analysis

For this investigation, unless otherwise specified, data analysis was done in R with R studio (Table A1).

2.10.1 Quantitative sequencing

Quantitative sequencing was used to determine the presence and frequency of the I1017F SNP in *CHSI*, that is associated with etoxazole resistance. The DNA sequences provided by Robarts Research Institute were analyzed using the Staden package (Staden, 1996; <https://sourceforge.net/projects/staden/>). A 2014 study examining the effectiveness of quantitative sequencing for SNP quantification in TSSM found upper and lower limits of detection at a 95% confidence level of $93.3 \pm 3.2\%$ and $7.8 \pm 3.3\%$ (Kwon et al., 2014). While the exact accuracy of this technique with regards to the I1017F SNP was not examined, it is expected that there are upper and lower limits to detection. It should be noted that for this investigation an I1017F SNP frequency of 0% will be also referred to as below detection limit. A 100% frequency will only be referred to as such, since due to the continuous selection for etoxazole during the majority of the investigation, it is reasonable to conclude that the true frequency is at or very near 100%.

2.10.2 Dose response modelling

Data from ovicidal bioassays was used to construct a dose response curve for tested populations. The dose response curves in this investigation are regression models of an independent variable (etoxazole concentration) and the dependent variable (mortality) (Ritz et al., 2015). The mortality was the percent of the total population that was found to be dead. Lethal concentration (LC) values are taken from the dose response models. Resistance ratios (RR) in this investigation are the LC50 value of a TSSM population divided by the LC50 value of a susceptible control. Dose response modelling was done in R with the package (drm).

$$\text{Resistance ratio (RR)} = \frac{\text{LC50 of TSSM}}{\text{LC50 of susceptible TSSM}}$$

2.10.3 Genetic modelling

The modeling of different parameters of a population under a selection pressure was done using the (learnPopGen) package in R. The hypothetical models are based on diploid species. TSSM are a haplodiploid (arrhenotokous parthenogenesis) species, however, the models serve to demonstrate the forces that can influence the buildup of a recessive allele.

3 Results

3.1 TSSM population history

In February 2019 the TSSM colonies, collected in the fall of 2018, were genotyped for the I1017F SNP. All TSSM populations had a 100% frequency of the SNP and were predicted to be highly resistant to etoxazole. Etoxazole bioassays took place in December of 2019, 10 months after samples were taken for genotyping. It was found that most populations were susceptible to etoxazole. Subsequent genotyping in March 2020 showed a significant drop in the frequency of the I1017F SNP (Table 3.1). The TSSM populations were kept bean leaves with no etoxazole exposure. In the absence of selective pressure for etoxazole resistance the I1017F SNP was gradually lost. Literature indicates the I1017F SNP carries a metabolic and fitness cost (Bajda et al., 2018). It was concluded that mites that did not carry the I1017F SNP were able to outcompete the mites with the I1017F SNP within the populations. The result was the loss of the I1017F SNP and etoxazole susceptibility.

Table 3.1: TSSM I1017F genotype shift without etoxazole selection (12 months).

Mite Population	I1017F Frequency	
	Feb. 2019	March 2020
01	100%	0%*
02	100%	50%
04	100%	0%*
05	100%	0%*
06	100%	0%*
08	100%	0%*
09	100%	0%*
10	100%	0%*
11	100%	0%*
13	100%	0%*
14	100%	0%*
16	100%	0%*
17	100%	0%*
18	100%	0%*
19	100%	0%*

* Below detection threshold

To reestablish a correlation between mite resistance to etoxazole and high frequency of I1017F SNP, populations were put on the etoxazole selection. A subset of 15 (plus 1 lab population, LND) of the 18 original mite populations were chosen. These populations were used throughout my investigation. A full history of the work with these populations (including the thesis investigation and prior work) is depicted in Figure 3.1.

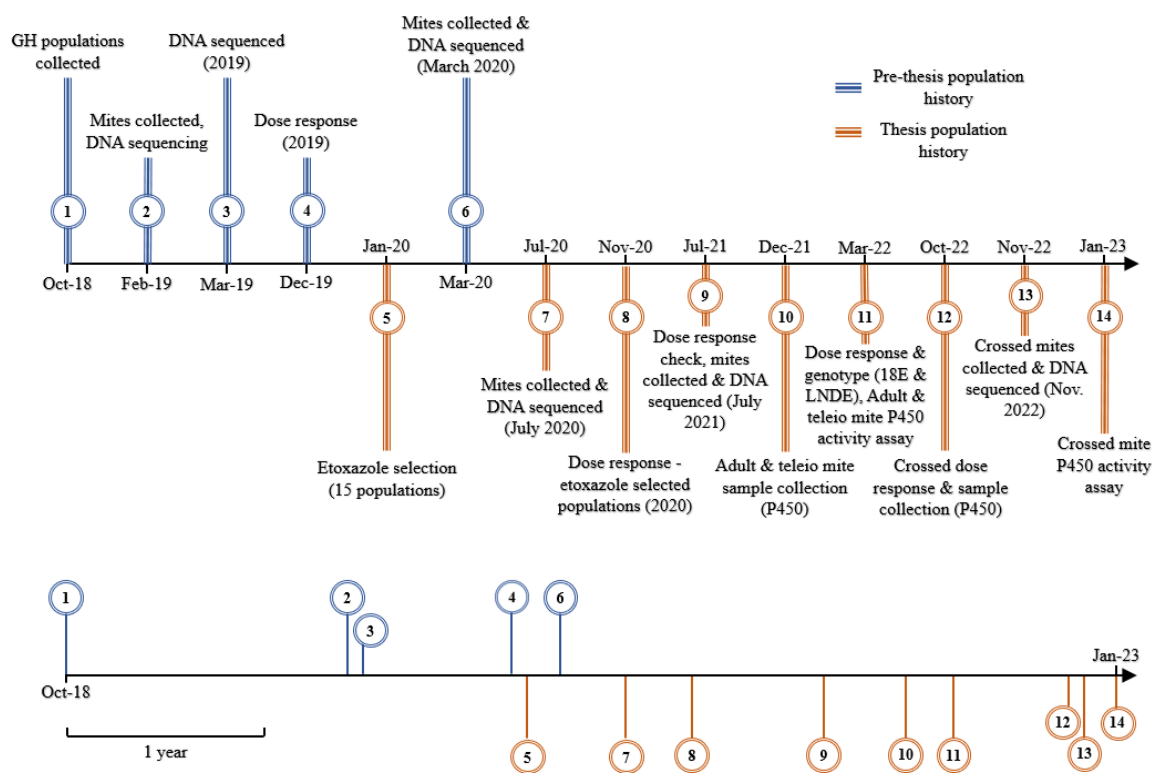


Figure 3.1: Etoxazole mite population history. History of work on greenhouse collected mite populations regarding etoxazole resistance. Sequential timeline (top) and scaled timeline (bottom).

3.2 Etoxazole selection

The concentration of etoxazole used for selection was 0.02 mg/L. This was the approximate LC₉₀ value (0.0196 mg/L) of the LND mite population during initial etoxazole testing in December 2019. The LC₉₀ value was derived based on the ovicidal assays (section 2.5) where leaf disks with attached eggs were submerged in etoxazole solutions for 5 seconds. However, leaf dipping with attached eggs would be impractical for

selection as it would wash off mobile stages of TSSM. The selection protocol (section 2.4) used leaves pretreated with etoxazole prior to their use in maintenance of TSSM populations. Oviposition of eggs onto etoxazole treated leaves is expected to result in a significantly lower dose of etoxazole being delivered to the egg than when eggs were submerged into an etoxazole solution. A test of this selection pressure showed that egg mortality on leaves pretreated with etoxazole did not statistically differ from untreated controls (Figure 3.2). However, despite the lack of a significant difference relative to the control, pretreatment of leaves did provide a selection pressure. This was evident by the eventual buildup in the I1017F SNP in all populations under continuous selection. Thus, the etoxazole selection pressure was mild, but continuously present during the maintenance of the selected TSSM populations during this investigation.

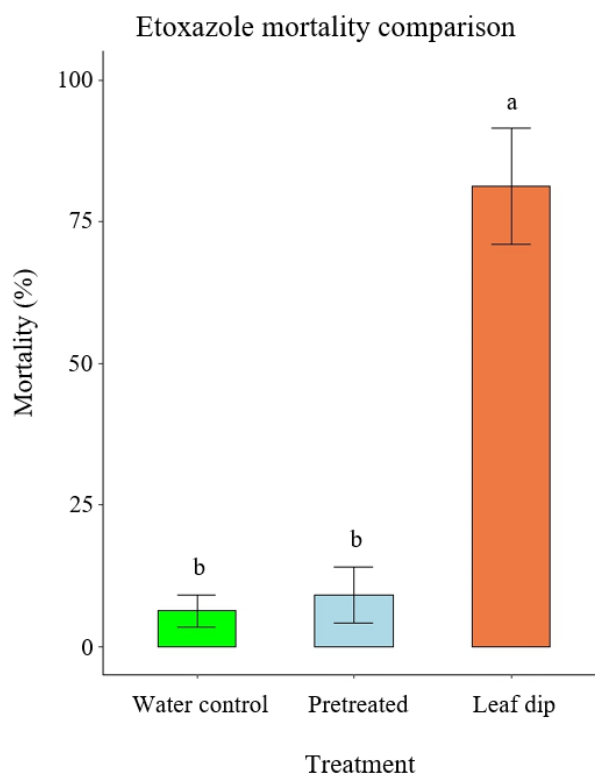


Figure 3.2: Etoxazole mortality comparison. Ovicidal mortality of LND population on untreated control leaf disks, etoxazole pretreated leaf disks, and leaf disks submerged (leaf dip) for 5 seconds. Etoxazole concentration used was 0.02 mg/L. Mean mortality \pm 95% confidence interval. Experiment performed in 3 independent trials. P450 activities with or sharing the same letter are not significantly different.

Table 3.2: ANOVA: etoxazole mortality comparison data

	Sum of squares	Degrees of freedom (df)	Mean square	F value	Significance (P value)
Treatment	4.269	2	2.1345	187.5	$< 2.00 \times 10^{-16}$
Residuals	0.364	32	0.0114		

Table 3.3: Tukey HSD table: etoxazole mortality comparison data

Treatments	Mean difference	95% Confidence interval		Significance (P value)
		Lower bound	Upper bound	
Pretreated: Control	0.0282	-0.0812	0.1377	8.02×10^{-1}
Leaf dip: Control	0.7488	0.6419	0.8559	1.00×10^{-13}
Leaf dip: Pretreated	0.7206	0.6112	0.8301	1.01×10^{-13}

3.2.1 Etoxazole resistance monitoring (Jan'20 - Jul'21)

This investigation monitored mite resistance to etoxazole over time of populations collected from commercial greenhouses. To reestablish a correlation between mite resistance to etoxazole and high frequency of I1017F SNP, populations were put on the etoxazole selection. The etoxazole selected populations, including the lab population LND, were genotyped for the I1017F SNP 7 months later and were retested for etoxazole resistance by ovicidal bioassay after 11 months. Etoxazole selection was successful in rescuing the I1017F SNP in many greenhouse populations (Table 3.2 and Figure 3.3). The lab LND population, despite not having detectable I1017F SNP initially, accumulated ~50% of the I1017F SNP frequency. This suggests that I1017F SNP was present in the LND population but was below detection level. Among selected mite populations, 10 populations with intermediate to high levels of etoxazole resistance had I1017F SNP frequencies ranging from 40% to 90%. The other 6 populations retained low frequencies of the I1017F SNP, (01E, 09E, 10E, 13E, 17E, and 18E) with frequencies of (30%, 15%, 15%, 0%, 0%, and 0%) respectively. These populations had a low level of resistance to etoxazole. I hypothesized that they may have an alternative method of resistance that may include metabolic detoxification. It was decided that these 6 etoxazole selected populations would be carried forward, along with the etoxazole selected LND population (LNDE).

Table 3.4: Etoxazole selected mite populations I1017F genotype shift.

Mite Population	I1017F Frequency		
	Feb. 2019	March 2020	July 2020
01E	100%	0% *	30%
02E	100%	50%	90%
04E	100%	0% *	30%
05E	100%	0% *	45%
06E	100%	0% *	70%
08E	100%	0% *	80%
09E	100%	0% *	15%
10E	100%	0% *	15%
11E	100%	0% *	90%
13E	100%	0% *	0% *
14E	100%	0% *	75%
16E	100%	0% *	40%
17E	100%	0% *	0% *
18E	100%	0% *	0% *
19E	100%	0% *	40%
LNDE	100%	0% *	50%

* Below detection threshold

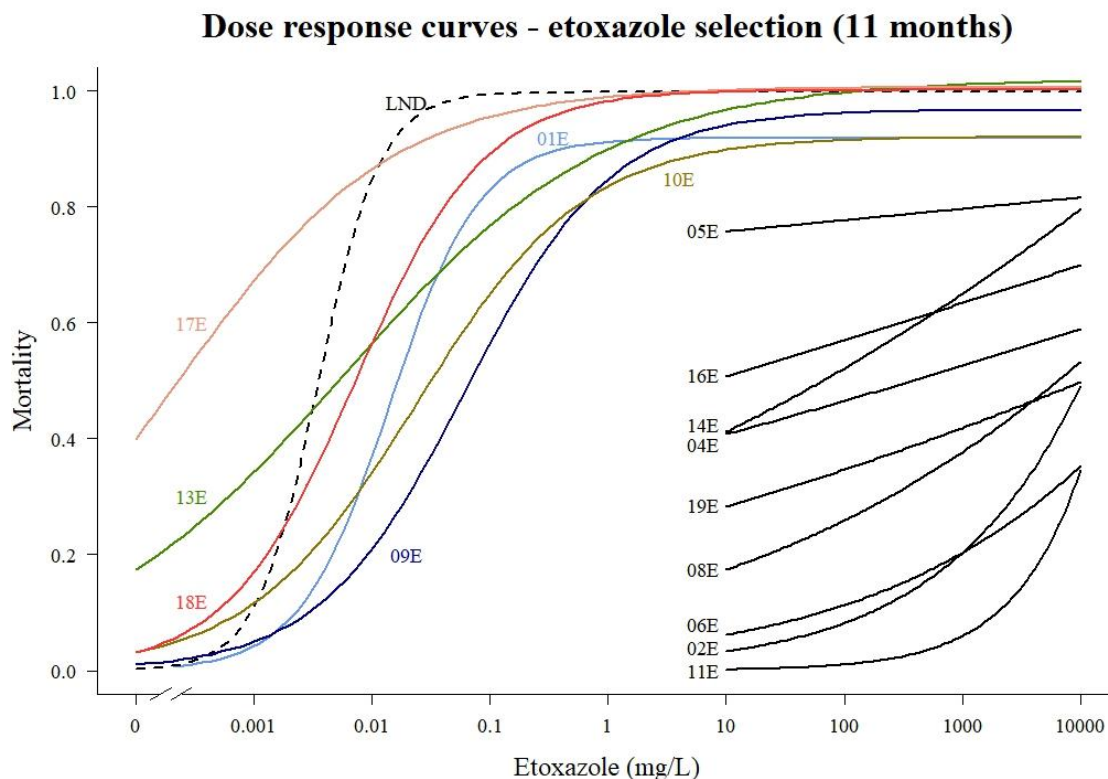


Figure 3.3: Dose response curves – etoxazole selection (11 months). Mortality versus etoxazole concentration data of TSSM populations that were subjected to etoxazole selection for 11 months (Jan. 2019 – Nov. 2020). Etoxazole concentrations used ranged from 0.001-10,000mg/L, increasing by a factor of 10, with a water control.

The 6 populations (01E, 09E, 10E, 13E, 17E, and 18E) were kept on the same etoxazole selection protocol as before and genotyped for I1017F after an additional 11 months of etoxazole selection (19 months total). Etoxazole selection had increased the I1017F SNP frequency in 4 of the 6 populations (01E, 10E, 13E, and 17E), with 09E and 18E having an I1017F frequency below detection (Table 3.3). A limited dose response check of the 6 etoxazole selected populations was done at 1 mg/L and 10 mg/L concentrations of etoxazole. There was a shift towards resistance in all 6 populations (Figure 3.4). The shift in resistance to etoxazole was also present in both 09E and 18E populations even though they did not have detectable presence of the I1017F SNP.

Table 3.5: Etoxazole selected mite populations after 19 months.

Mite Population	I1017F Frequency		
	March 2020	July 2020	July 2021
01E	0%*	30%	55%
09E	0%*	15%	0%*
10E	0%*	15%	33%
13E	0%*	0%*	70%
17E	0%*	0%*	55%
18E	0%*	0%*	0%*

* Below detection threshold

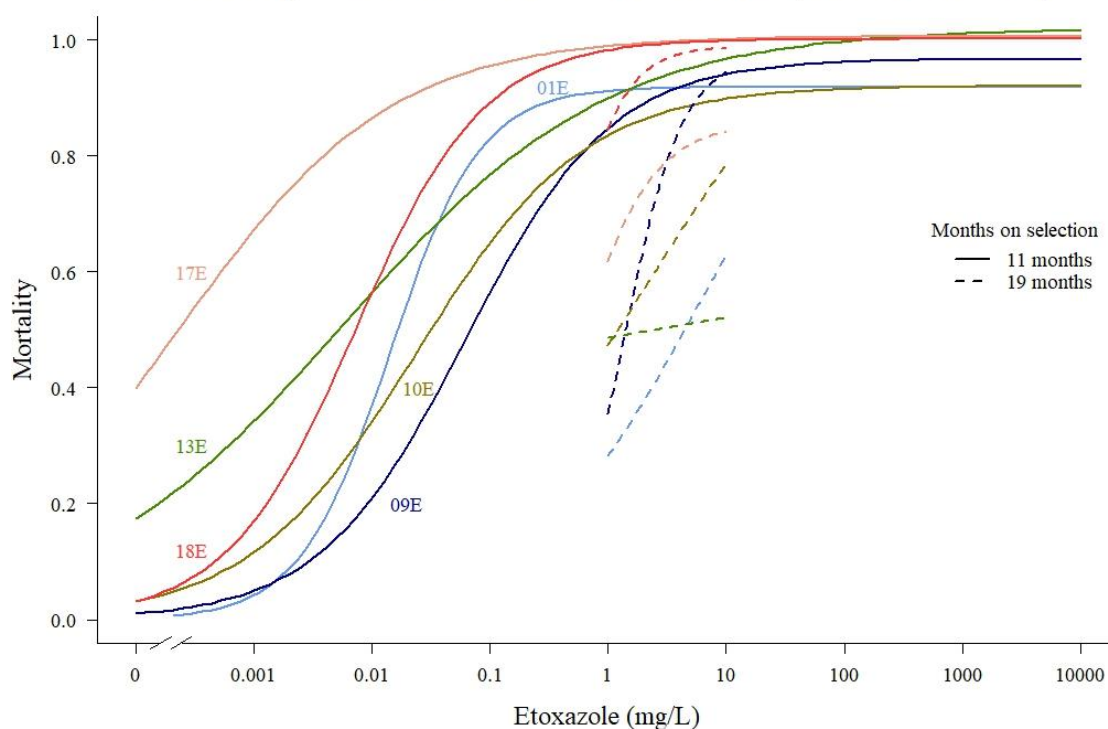
Dose response curves - etoxazole selection (11 & 19 months)

Figure 3.4: Dose response curves – etoxazole selection (11 & 19 months). Mortality versus etoxazole concentration data of TSSM populations that were subjected to selection to etoxazole for 11 months (dashed lines) and 19 months (solid lines). Etoxazole concentrations used at 11 months ranged from 0.001-10,000 mg/L, increasing by a factor of 10, with a water control. At 19 months etoxazole concentrations of 1 mg/L and 10 mg/L were used.

The final dose response assay was performed in March 2022. At this time, I focused on populations 18E and LNDE. The population 18E did not have a detectable I1017F SNP over a period of 31 months (from Jan. 2019 to Jul. 2021). However, by March 2022, both 18E and LNDE had become highly resistant to etoxazole (Figure 3.5). These populations were genotyped and found that they both had I1017F SNP frequencies of 100% (Table 3.4). The resistance to etoxazole was so extreme that the data could not be modeled to determine reliable LC values. The LNDE and 18E mite populations had become functionally immune to the toxic effects of etoxazole.

Dose response - LNDE & 18E (Feb-Mar, 2022)

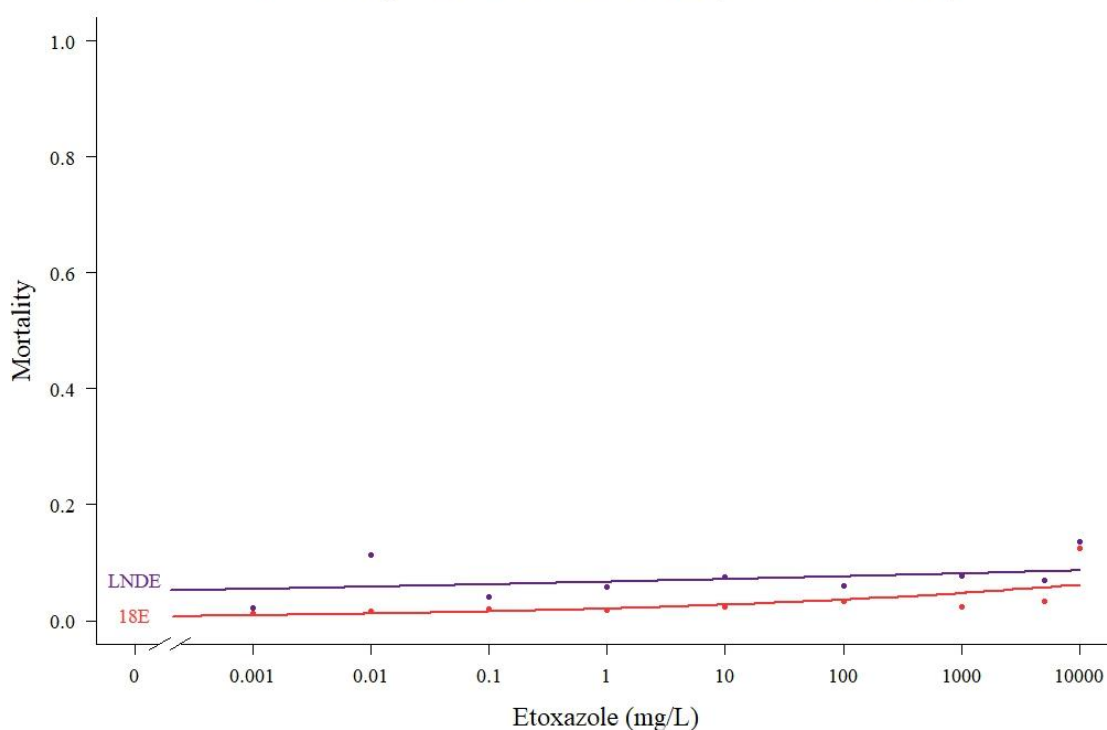


Figure 3.5: Dose response - LNDE & 18E (Feb-Mar, 2022). Mortality versus etoxazole concentration data of TSSM populations that were subjected to selection to etoxazole for 31 months. Etoxazole concentrations used ranged from 0.001-10,000 mg/L, increasing by a factor of 10, including 5000 mg/L, with a water control.

Table 3.6: Etoxazole selected mite populations after 31 months.

Mite Population	I1017F Frequency
	March 2022
LND	0%*
LNDE	100%
18E	100%

* Below detection threshold

3.3 P450 activity: LND, LNDE and 18E mite populations

A single trial preliminary survey of P450, esterase and GST activities in 01E, 09E, 10E, 13E, 17E, 18E, LNDE, and LND mite populations, revealed that there were no significant differences in the esterase or GST activities. However, the P450 activity of population 18E was elevated compared to the susceptible LND population and other etoxazole-selected populations. Thus, I performed a more robust P450 assay on 18E, LNDE and LND mite populations. Female TSSM at the adult and teleiochrysalis stages were used. Synchronized populations of LND, LNDE, and 18E were created and sampled in triplicate. The protein was quantified by Bradford assay and was used for a P450 activity assay.

The results confirmed that 18E mites showed a significant increase in P450 activity in both developmental stages relative to P450 activity in LND and LNDE (Figure 3.6). Adult females of 18E showed a statistically significant increase of 7-HFC production over a 30-minute reaction time than either LND or LNDE (Table 3.8). Similar to the adult females, 18E teleios showed a statistically significant increase in 7-HFC production relative to teleios from LND or LNDE. There was no significant difference in 7-HFC production between LND and LNDE at either the adult or teleio developmental stage.

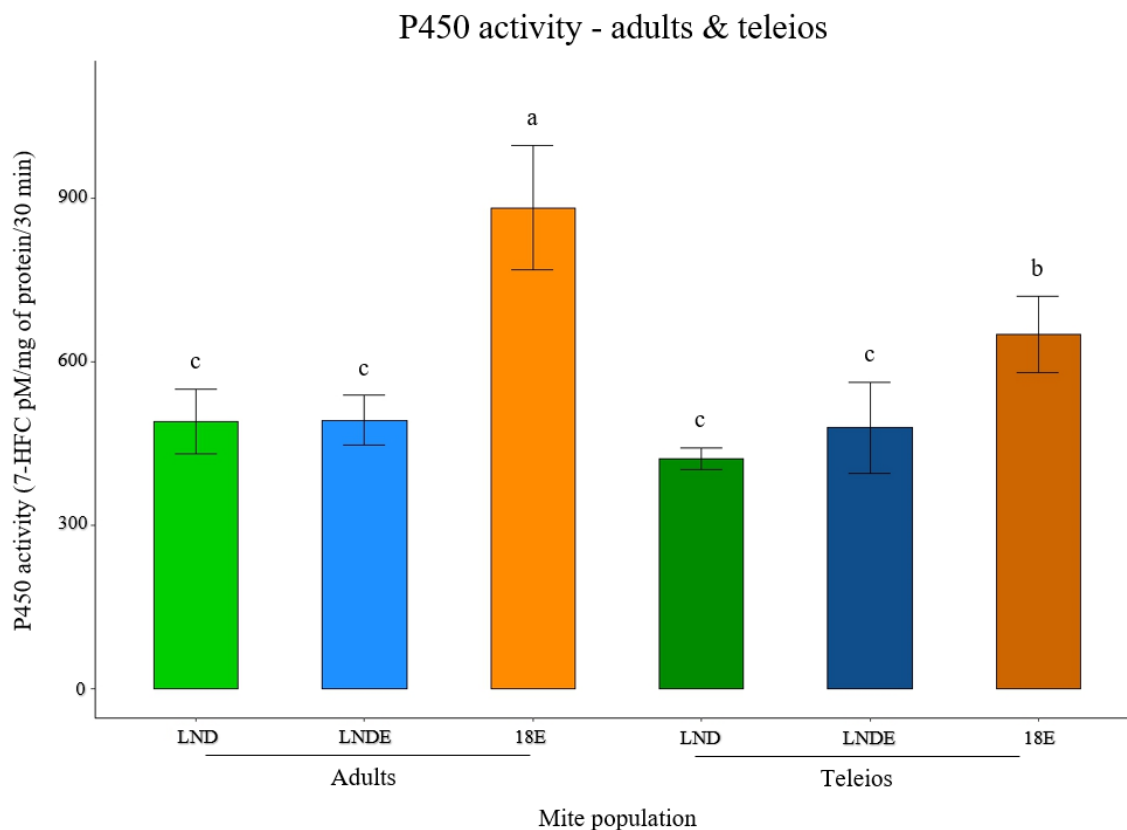


Figure 3.6: P450 activity – adults & teleios. P450 enzyme activity of synchronized TSSM populations of LND, LNDE, and 18E. Populations were sampled at the adult and teleiochrysalis stage. Mean concentration of 7-HFC \pm 95% confidence interval. The experiment was performed in 3 independent replicas. P450 activities with or sharing the same letter are not significantly different.

Table 3.7: ANOVA: P450 activity – adults & teleios data

	Sum of squares	Degrees of freedom (df)	Mean square	F value	Significance (P value)
Population	1312014	5	262403	30.22	1.31×10^{-13}
Residuals	408161	47	8684		

Table 3.8: Tukey HSD: P450 activity – adults & teleios data

Populations	Mean difference	95% Confidence interval		Significance (P value)
		Lower bound	Upper bound	
Adults				
LNDE: LND	1.9393	-132.5694	136.4480	1.00×10^0
18E: LND	392.2239	257.7151	526.7326	3.95×10^{-10}
18E: LNDE	390.2846	259.7919	520.7772	1.86×10^{-10}
Teleios				
LNDE: LND	56.0583	-74.4343	186.5510	7.96×10^{-1}
18E: LND	227.0141	96.5214	357.5068	6.71×10^{-5}
18E: LNDE	170.9558	40.4631	301.4484	4.00×10^{-3}

3.4 Analysis of genetic crossing method

To further examine the requirement of P450s in mite resistance to etoxazole I focused on the 18E population that showed high P450 activity. However, by this time, the 18E population became homozygous for the mutation in *CHSI*, which on its own confirms a high level of resistance to etoxazole. Thus, to investigate the role of P450s on mite etoxazole resistance I had to remove the effect of the target-site mutation. As target-site mutation in *CHSI* is recessive, crossing 18E with susceptible LND mites will result in heterozygosity at *CHSI* locus, eliminating the effect of target-site mutation on mite etoxazole resistance status. It was hoped that any increased P450 activity would carry through the crossing, though it was not assured.

F1 hybrids were made between 18E and LND mites, and between LNDE with LND mites. A small-scale pilot compared the crossing methods, ♀ (LND, LNDE, 18E) × ♂LND (Figure 3.7A) and ♀LND × ♂ (LND, LNDE, 18E) (Figure 3.7B), or LND male crossing and LND female crossing, respectively. The theoretical genotypes, with regards to *CHSI*, of females from either method are identical. Crosses between susceptible LND (AA) mites and resistant LNDE (aa) or 18E (aa) mites yields heterozygous female offspring. The resulting male offspring differ between methods since haploid males result from unfertilized eggs from the female parent. The LND male crossing method will yield etoxazole resistant males when crossed with LNDE or 18E females, while the LND female crossing method will result in etoxazole susceptible male offspring (Table 3.5 and Table

3.6). If the genetic crossing is successful, the F1 hybrids will show an etoxazole resistance status similar to that of a susceptible LND control.

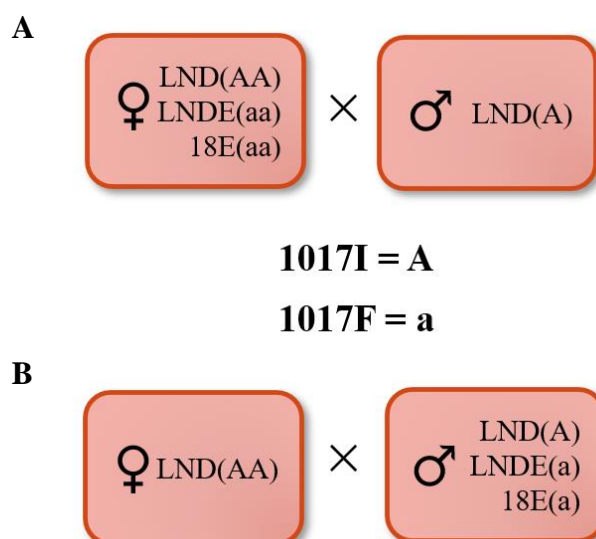


Figure 3.7: Genetic crossing methods. (A) = wildtype etoxazole susceptible dominant allele, 1017I, (a) = mutant etoxazole resistant recessive allele, 1017F. A) ♀LND, ♀LNDE, and ♀18E crossed with ♂LND, B) ♀LND crossed with ♂LND, ♂LNDE, and ♂18E.

Table 3.9: LND male crossing theoretical outcome.

Cross	F1 Offspring	
	Female	Male
♀LND × ♂LND	AA	A
♀LNDE × ♂LND	Aa	a
♀18E × ♂LND	Aa	a

Table 3.10: LND female crossing theoretical outcome.

Cross	F1 Offspring	
	Female	Male
♀LND × ♂LND	AA	A
♀LND × ♂LNDE	Aa	A
♀LND × ♂18E	Aa	A

The protocol for the genetic crossing experiment was chosen after a limited pilot of the two methods. The data yielded dose response curves of distinctly different shapes. The LND male method produced a dose response curve for the ♀LNDE × ♂LND and ♀18E × ♂LND F1 hybrids that plateaued. The plateaus were expected, due to the parentage of the F1 hybrid males. In the LND male method the F1 males are a result of unfertilized eggs from LNDE or 18E females. This results in the F1 males possessing the I1017 SNP and being highly resistant to etoxazole. The resistant F1 male offspring effectively cap the maximum mortality to no more than the total percent of the population composed of susceptible F1 female mites (Figure 3.8). The LND female crossing method produced a more typical dose response curve. This method allows the mortality to reach 100% of the treated mite population for both F1 hybrids and ♀LND × ♂LND (Figure 3.9).

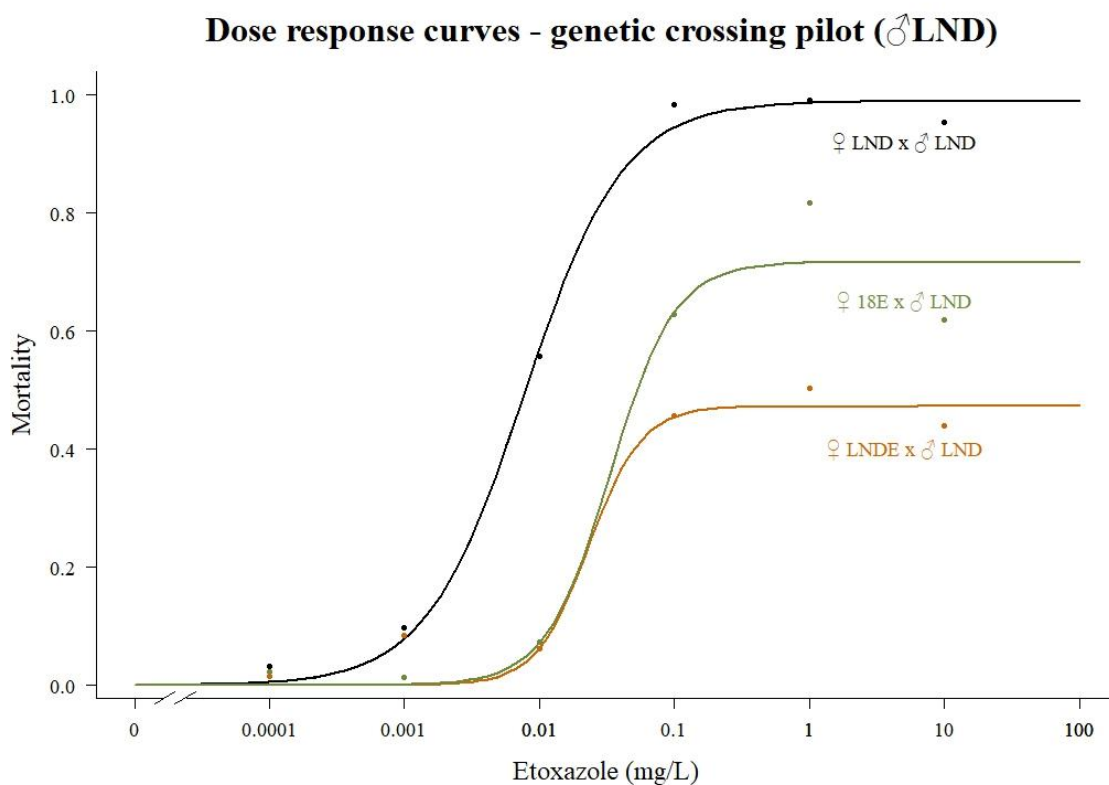


Figure 3.8: Dose response curves – genetic crossing pilot (♂LND). A small-scale pilot dose response curve (1 replica) of a crossing method utilizing males from the LND mite colony to produce F1 hybrids with LNDE and 18E.

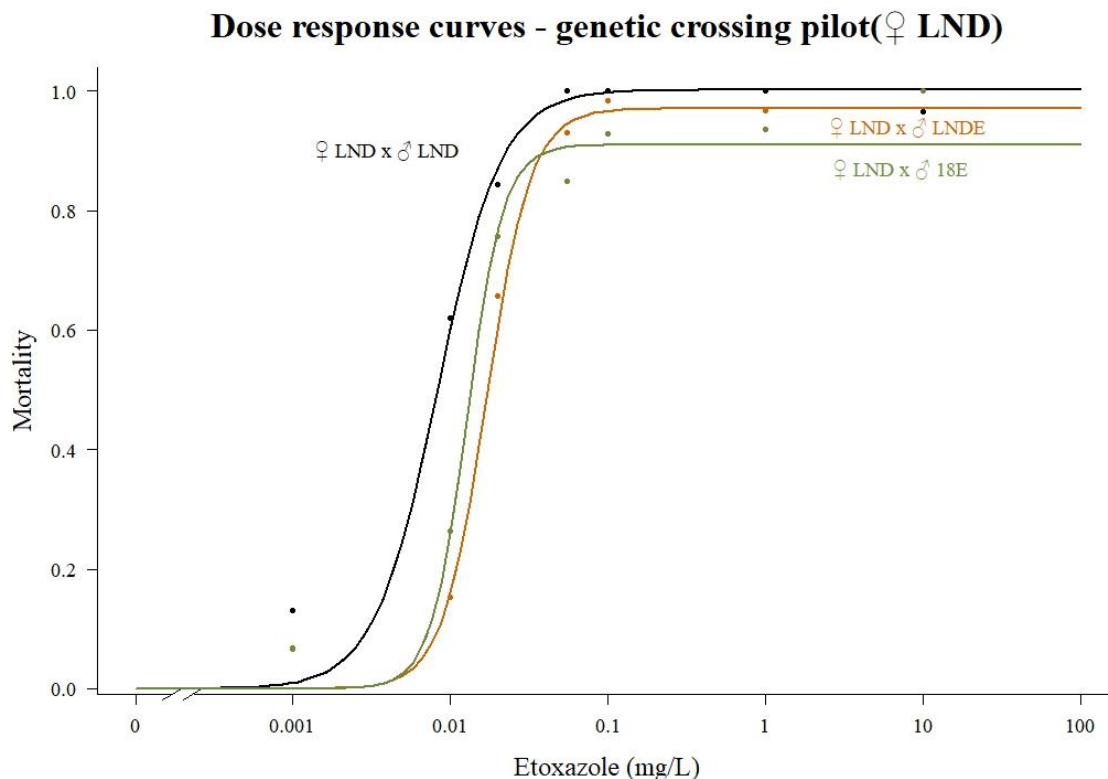


Figure 3.9: Dose response curves – genetic crossing pilot (♀LND). A small-scale pilot dose response curve (1 replica) of a crossing method utilizing females from the LND mite colony to produce F1 hybrids with LNDE and 18E mites.

The LND male method did offer an advantage of the dose response curve only showing mortality from F1 females. However, the rates of males within the populations limited the maximum mortality the curves could reach, as they are the result of unfertilized eggs from female mites homozygous for the *CHS1* with the I1017F mutation (Figure 3.8). It was found that ratio of males to females within populations varied from LNDE and 18E, and between trials. Males can represent as little as 15% of the population or exceed 50% (Table 3.7). Data from the LND male method produced dose response curves that were a poor fit the regression model of the (drc) package in R, revealed by the modelFit () function within the (drc) package. The LND female method produced data that was an ideal fit for modelling of a dose response curve using (drc), and thus, this method was chosen for the full genetic crossing experiment.

Table 3.11: Ratio of males in genetic crossing experiment water controls

Mite Population	% Male of water controls		
	Trial 1	Trial 2	Trial 3
♀LND × ♂LND	49.3%	55.6%	54.1%
♀LND × ♂LNDE	36.8%	49.3%	30.4%
♀LND × ♂18E	24.4%	54.2%	49.6%
♀LNDE × ♂LNDE	46.3%	68.1%	53.4%
♀18E × ♂18E	15.8%	14.2%	25.5%

The full-scale genetic crossing experiment was done using a positive control for mortality of a ♀LND × ♂LND “cross” and negative controls of ♀LNDE × ♂LNDE and ♀18E × ♂18E. These “crosses” underwent the same synchronization and genetic crossing protocol used to generate the F1 hybrids. This ensured that manipulation and treatment of all mites involved were identical in the genetic crossing experiment.

3.5 Genetic crossing experiment

3.5.1 Dose response: ♀LND × ♂LND

The positive control dose response curve for mortality was the ♀LND × ♂LND dose response curve. The data behaved as expected with the mortality quickly rising and reaching a plateau well before active ingredient (ai) field rates of 30 – 60 mg/L (Figure 3.10). The susceptible LND mites were found to have an etoxazole LC90 of 0.03091 mg/L. Despite the susceptible nature of the LND mites, surviving mites were found on leaf disks at the higher concentrations tested of 1 mg/L and 10 mg/L of etoxazole. The survival of mites from a susceptible population at these concentrations does not meet expectations, suggesting a mechanism for etoxazole resistance has become present with the LND population.

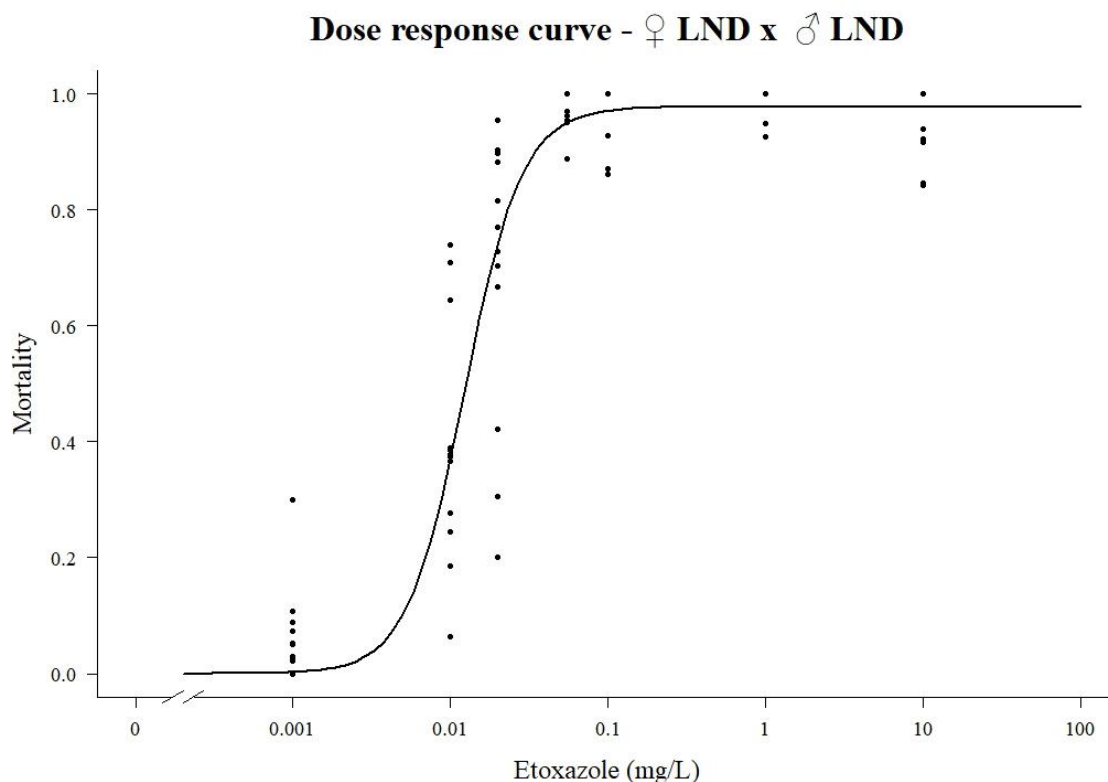


Figure 3.10: Dose response curve - ♀LND × ♂LND. Mortality versus etoxazole concentration (mg/L) data for LND females fertilized by LND males. Individual data points represent data from 1 leaf disk, with 4 leaf disks per trial with 3 trials. LC90 = 0.03091 mg/L, LC50 = 0.01230 mg/L, LC10 = 0.00489 mg/L.

3.5.2 Dose response: ♀LND × ♂LNDE

The genetic cross of ♀LND × ♂LNDE showed a resistance profile of a susceptible mite population (Figure 3.11). The model reaches a plateau of mortality under 100% mortality. There was variation in mortality at the higher etoxazole concentrations of 1 mg/L and 10 mg/L. The genetic cross of ♀LND × ♂LNDE had an etoxazole LC90 of 0.04557 mg/L with a resistance ratio (RR, see details in 2.10.2) of 1.537.

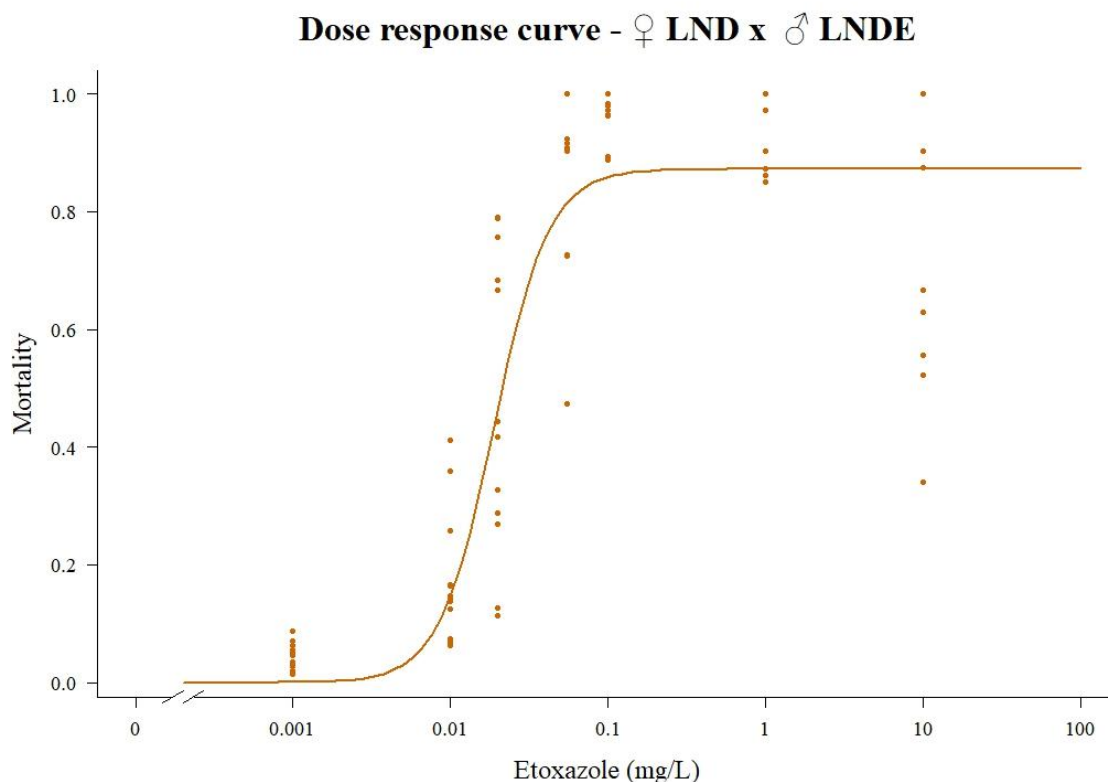


Figure 3.11: Dose response curve - ♀LND × ♂LNDE. Mortality versus etoxazole concentration (mg/L) data for ♀LND × ♂LNDE F1 hybrids. Individual data points represent data from 1 leaf disk, with 4 leaf disks per trial with 3 trials. Etoxazole concentrations used at ranged from 0.001-10,000 mg/L, increasing by a factor of 10, with additional concentrations of 0.02 mg/L and 0.055 mg/L, with a water control. LC90 = 0.04557 mg/L, LC50 = 0.01891 mg/L, LC10 = 0.00785 mg/L.

3.5.3 Dose response: ♀LND × ♂18E

The genetic cross of ♀LND × ♂18E showed a resistance profile of a susceptible mite population, similar to the genetic cross of ♀LND × ♂LNDE (Figure 3.12). The model of ♀LND × ♂18E reaches a plateau of mortality under 100% mortality. There was variation at the higher etoxazole concentrations of 1 mg/L and 10 mg/L. The genetic cross of ♀LND × ♂18E had a LC90 of 0.05480 mg/L with a RR of 1.405.

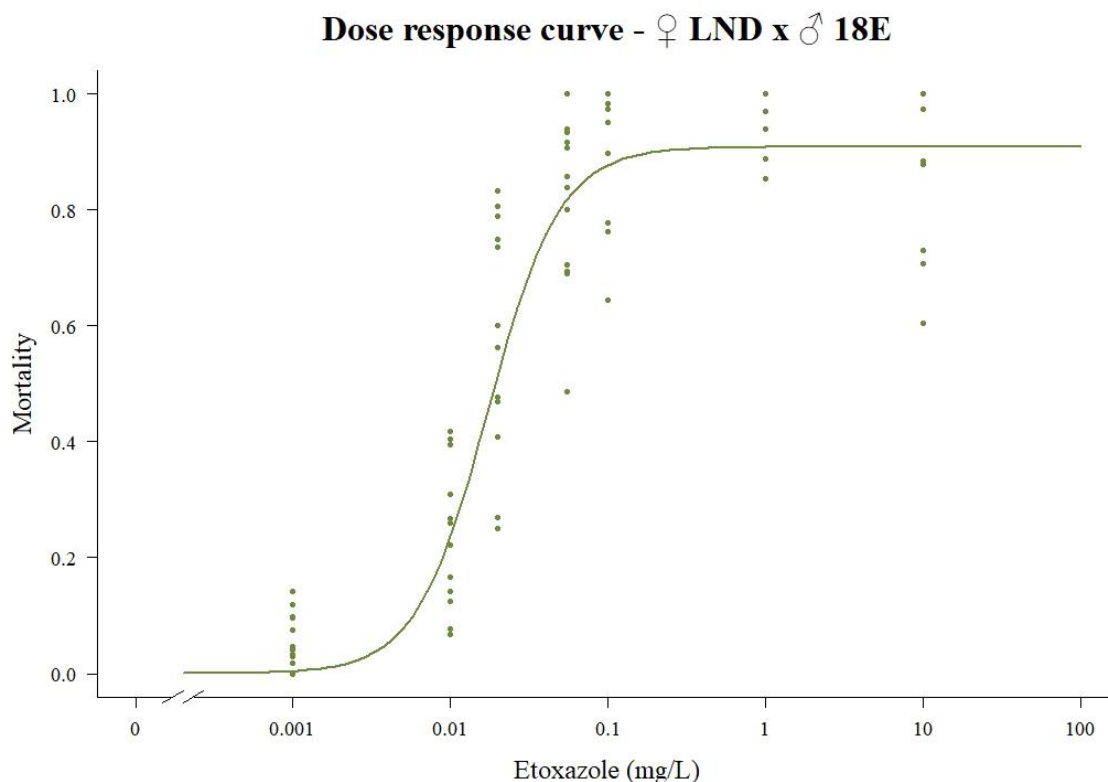


Figure 3.12: Dose response curve - ♀LND × ♂18E. Mortality versus etoxazole concentration (mg/L) data for ♀LND × ♂18E F1 hybrids. Individual data points represent data from 1 leaf disk, with 4 leaf disks per trial with 3 trials. Etoxazole concentrations used at ranged from 0.001-10,000 mg/L, increasing be a factor of 10, with additional concentrations of 0.02 mg/L and 0.055 mg/L, with a water control. LC90 = 0.05480 mg/L, LC50 = 0.01729 mg/L, LC10 = 0.00545.

3.5.4 Combined dose responses plot

Figure 3.13 shows the dose response curves made of both F1 hybrids plotted with the susceptible positive control and resistant negative controls. Even though the F1 hybrids of ♀LND × ♂LNDE and ♀LND × ♂18E show a shift toward the resistance, their etoxazole resistance status was similar to the ♀LND × ♂LND control. LC90 values for the F1 hybrids (♀LND × ♂LNDE LC90 = 0.0456 mg/L, ♀LND × ♂18E LC90 = 0.0548 mg/L) are well under the field rate of etoxazole (30-60 mg/L). Furthermore, the `compPerm ()` function of the `(drc)` was used to compare the slopes of the dose response curves and no statistically

significant difference were found between the slope of the ♀LND × ♂LND control and the slopes of the F1 hybrids (♀LND × ♂LND : ♀LND × ♂LNDE, $t = 0.2124$, $P = 0.8320$) (♀LND × ♂LND : ♀LND × ♂18E, $t = -0.8500$, $P = 0.3961$). The etoxazole concentrations used for the F1 hybrids and ♀LND × ♂LND control were 0.001, 0.01, 0.02, 0.055, 0.1, 1, and 10 mg/L, with 10 and 100 mg/L used for resistant negative controls. The negative controls behaved as expected, showing immunity to etoxazole.

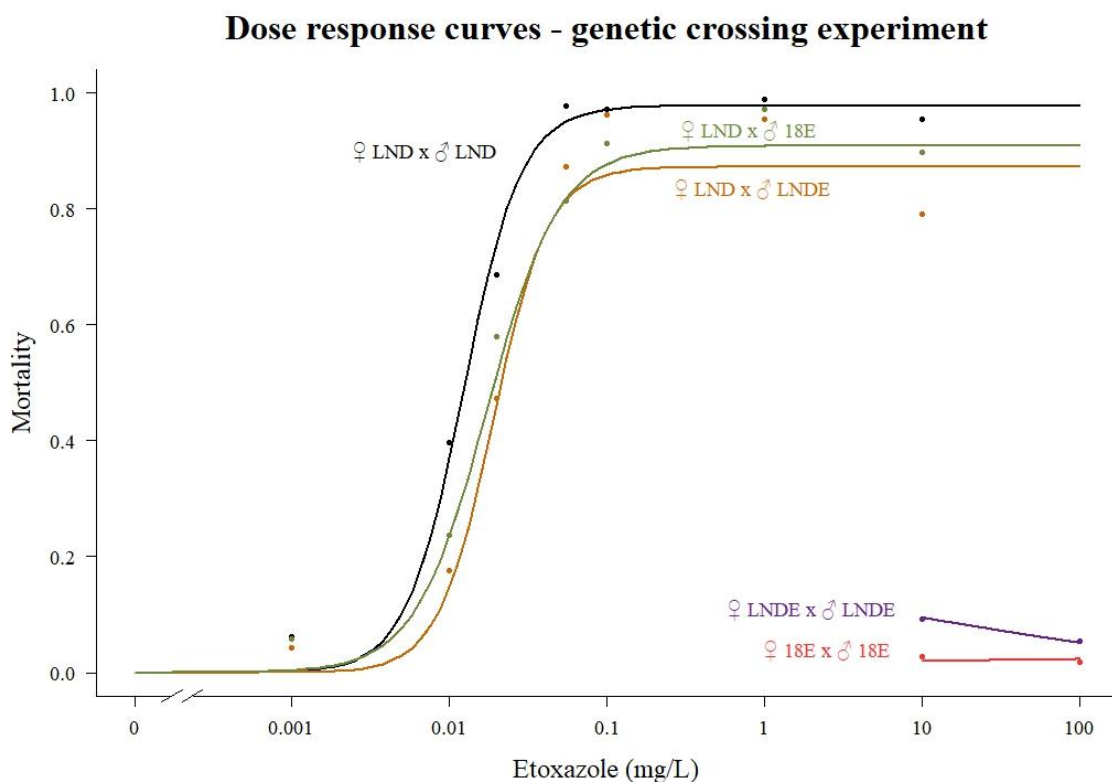


Figure 3.13: Dose response curve – genetic crossing experiment. Mortality versus etoxazole concentration (mg/L) data for F1 hybrids (♀LND × ♂LNDE and ♀LND × ♂18E), a ♀LND × ♂LND positive control, and negative controls (♀LNDE × ♂LNDE and ♀18E × ♂18E). Etoxazole concentrations used at ranged from 0.001-10,000 mg/L, increasing by a factor of 10, with additional concentrations of 0.02 mg/L and 0.055 mg/L, with a water control. Data points represent the average mortality of leaf disks.

3.5.5 F1 hybrids deviation from expected genotype

The expected I1017F SNP frequency of the ♀LND × ♂LND control is 0%. In addition, the F1 hybrid females are expected to be heterozygous for the I1017F SNP, resulting in a 50% I1017F SNP frequency. However, there is a slight shift towards resistance of the F1 hybrid dose response curves and both curves plateaued below the curve of the ♀LND × ♂LND susceptible control (Figure 3.13). The susceptible control of ♀LND × ♂LND also displayed a curve that did not reach 100% mortality. This suggested that there were individuals within the ♀LND × ♂LND controls and F1 hybrid populations that were fully resistant to etoxazole.

Inspection of the data points in Figure 3.10, of the ♀LND × ♂LND control, shows that some mites on leaf disks treated with etoxazole at concentrations of 1 mg/L and 10 mg/L did not have 100% mortality. In isolation, this could be explained as expected variation within experimental results. However, experience prior to this investigation with etoxazole ovicidal bioassays and the LND population suggested that this variation was unusual. Examination of the data from previous etoxazole dose responses of the LND population prior to the genetic crossing experiment showed that mortality at etoxazole concentration above 0.1 mg/L is consistently uniform at 100% with only very rare exceptions. During the genetic crossing experiment the mortality of LND was consistently high at 0.1 mg/L to 10 mg/L etoxazole, but rarely at 100%.

In order to check the I1017F SNP frequency of mites that survived etoxazole treatment, additional trials of both F1 hybrids and the ♀LND × ♂LND control were completed where survivors were genotyped. Adult females from the lab colony of LND were also sampled. Additional trials of F1 hybrids used etoxazole concentrations at 0.02 mg/L and 0.055 mg/L, with the ♀LND × ♂LND control at 0.02 mg/L, 0.055 mg/L, and 10 mg/L. The 0.02 mg/L and 0.055 mg/L etoxazole concentrations were chosen based on the dose response curve of the ♀LND × ♂LND control. Mortality varied at 0.02 mg/L then shifted to a consistently high mortality at 0.055 mg/L (Figure 3.10). This indicated survival of susceptible mites should be low at 0.055 mg/L and higher concentrations.

An examination of the I1017F SNP frequencies of mites that survived etoxazole treatment revealed a departure from the expected genotypes (Table 3.8). The ♀LND × ♂LND control showed the presence of the I101F SNP in all tested survivors, with frequencies of 100% at concentrations of 0.055 mg/L and 10 mg/L etoxazole. The F1 hybrids had an I1017F SNP frequency at or close to the expected 50% at 0.02 mg/L etoxazole. The frequency of the I1017F SNP increased to 100% at 0.055 mg/L etoxazole for the F1 hybrids. The 0.055 mg/L etoxazole concentration indicated that most, if not all, the mites in the ♀LND × ♂LND control and the F1 hybrids that survived at 0.055 mg/L or higher etoxazole concentrations carried the I1017F SNP at 100%. Other experiments were present in the incubation chamber where the genetic crossing experiments were incubated. Genotyping the LND colony gave insight into the possibility of contamination in the genetic crossing. The results suggest this was not a result of a contamination issue, but rather the result of the I1017 SNP within the LND colony. Females from the LND colony had an I1017F SNP frequency of 20%.

The purpose of the genetic crossing experiment was to create heterozygous F1 offspring. The presence of the I1017F SNP within the LND population served to interfere with that goal. Despite this, the genetic crossing protocol was largely successful in abolishing the resistance status conferred by two copies of the I1017F mutant allele by creating F1 hybrids that were predominantly heterozygous, as F1 hybrids were considered susceptible to etoxazole.

Table 3.12: Survivor genotype.

Mite Population	Etoxazole Concentration	I1017F Frequency
♀LND × ♂LND	0.02 mg/L	25%
♀LND × ♂LND	0.055 mg/L	100%
♀LND × ♂LND	10 mg/L	100%
♀LND × ♂LNDE	0.02 mg/L	55%
♀LND × ♂LNDE	0.055 mg/L	100%
♀LND × ♂18E	0.02 mg/L	50%
♀LND × ♂18E	0.055 mg/L	100%
LND colony	--	20%

3.5.6 P450 activity: genetically crossed populations

While performing etoxazole ovicidal bioassays as part of the genetic crossing experiment, the same adult female mites that oviposited F1 eggs (see section 2.6.3) were also used to oviposit large numbers of F1 eggs that were allowed to mature into adults for collection and use in Bradford and P450 activity assays.

It was unknown if the elevated level of P450 exhibited by the 18E population in March 2022 is retained in the ♀LND × ♂18E F1 hybrids. If the ♀LND × ♂18E F1 hybrid mites had retained a degree of increased activity of P450s and the genetic crossing abolished the target-site based etoxazole resistance by creating mites heterozygous for wildtype and mutant *CHS1* alleles, they would have provided an opportunity to observe possible metabolic resistance in a population without a background of etoxazole resistance due to the I1017F target-site mutation.

The results of the P450 assays indicated that the ♀18E × ♂18E (18E) population showed a statistically significant increase of P450 activity relative to the ♀LND × ♂LND (LND) (Table 3.14). The same trend was observed in the F1 hybrid of ♀LND × ♂18E, but not in the ♀LND × ♂LNDE F1 hybrid. The ♀LNDE × ♂LNDE (LNDE) population had a statistically significant increase of P450 activity from the LND population, but not the ♀LND × ♂18E or ♀LND × ♂LNDE F1 hybrid populations. The F1 hybrids showed no statistically significant difference from the LND susceptible control population (Figure 3.14).

Unfortunately, the ♀LND × ♂18E F1 hybrid population did not retain any apparent increased P450 activity. The ♀18E × ♂18E resistant control did retain a statistically significant difference from the ♀LND × ♂LND control, though the P450 activity was below the level of the previous P450 assay in Mar. 2022 and was no longer significantly higher than the LNDE population. As the elevated P450 activity was not retained in the ♀LND × ♂18E F1 hybrid or present in the ♀LND × ♂LNDE F1 hybrid, any shift in the dose response curves could not be attributed to increased P450 activity.

P450 activity – genetic crossing experiment

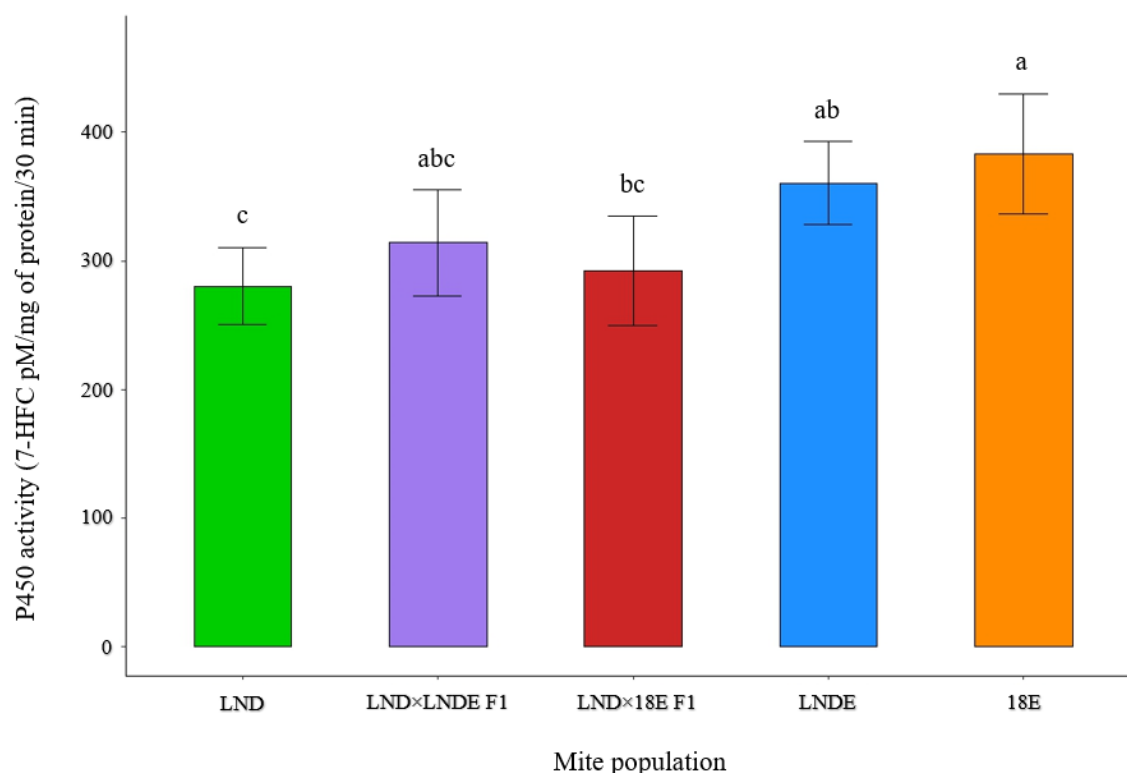


Figure 3.14: P450 activity – genetic crossing experiment. P450 activity of F1 hybrids of ♀LND × ♂LNDE and ♀LND × ♂18E and a positive control (♀LND × ♂LND) and negative controls (♀LNDE × ♂LNDE and ♀18E × ♂18E) of the genetic crossing experiment. Mean concentration of 7-HFC ± 95% confidence interval. Experiment performed in 5 independent replicas sampled at the adult stage. P450 activities with or sharing the same letter are not significantly different.

Table 3.13: ANOVA: P450 activity – genetic crossing experiment data.

	Sum of squares	Degrees of freedom (df)	Mean square	F value	Significance (P value)
Population	117613	4	29403	5.911	3.71×10^{-4}
Residuals	348221	70	4975		

Table 3.14: Tukey HSD: P450 activity – genetic crossing experiment data

Populations	Mean difference	95% Confidence interval		Significance (P value)
		Lower bound	Upper bound	
LNDE F1: LND	33.5881	-38.5276	105.7037	6.90×10^{-1}
18E F1: LND	11.6217	-60.4940	83.7373	9.91×10^{-1}
LNDE: LND	80.0375	7.9219	152.1532	2.21×10^{-2}
18E: LND	102.8430	30.7274	174.9586	1.45×10^{-3}
18E F1: LNDE F1	-21.9664	-94.0820	50.1492	9.13×10^{-1}
LNDE: LNDE F1	46.4495	-25.6662	118.5651	3.80×10^{-1}
18E: LNDE F1	69.2549	-2.8607	141.3706	6.58×10^{-2}
LNDE: 18E F1	68.4159	-3.6998	140.5315	7.12×10^{-2}
18E: 18E F1	91.2213	19.1057	163.3370	6.21×10^{-3}
18E: LNDE	22.8055	-49.3102	94.9211	9.01×10^{-1}

3.5.7 Genetic crossing experiment summary

The target-site based resistance to etoxazole of the LNDE and 18E parent mites was mostly abolished in the F1 hybrids of ♀LND × ♂LNDE and ♀LND × ♂18E. The F1 hybrids showed a slight shift, though this may be the result of the presence of the I1017F allele in the LND population. The presence of the I1017F allele in the LND population would result in F1 hybrid mites homozygous for the I1017F allele, giving a small number of F1 hybrid mites a target-site based resistance to etoxazole. No determination could be made for the possibility of P450s contributing to etoxazole resistance, as elevated P450 activity could not be isolated from a background of target-site based resistance.

4 Discussion

4.1 TSSM populations varying response to selection

The re-establishment of the I1017F SNP was not uniform in either speed or magnitude between different TSSM populations. The mild selection pressure during the continuous selection for etoxazole resulted in a longer time course for the buildup of the I1017F SNP than would be expected if a higher or increasing series of etoxazole concentrations were employed. This offered an opportunity to examine the populations that had a slower buildup of the I1017F SNP. Mite populations 01E, 09E, 10E, 13E, 17E, and 18E were initially selected for continued experimentation. These populations had a slower buildup of the I1017F SNP than other populations under selection. It was hypothesized that the buildup of the target-site mutation in *CHSI* may be slower in these populations because they possessed an alternative mechanism to resist etoxazole toxicity. If the mortality imposed by treatment with etoxazole was mitigated by metabolic resistance, then the selective pressure toward the re-establishment of the target-site mutation (I1017F SNP) is expected to be reduced. Under these circumstances, the buildup of the I1017F SNP within these populations will be slower or may not even occur. The preliminary survey of the enzymatic activity of esterases, GSTs, and P450s identified elevated P450 activity in the 18E population, suggesting that metabolic resistance to etoxazole may have developed.

In an effort to isolate any potential metabolic resistance from the high levels of resistance given by the I1017F target-site mutation, genetic crossing to create F1 hybrids heterozygous for *CHSI* alleles (I1017F/wildtype) was carried out. The causative genetic source of the elevated P450 activity of 18E was not known. Likewise, the nature of the inheritance of this elevated activity was unknown. It is possible the increased activity of P450s would not be retained in the F1 progeny, particularly if it was driven by a fully recessive source.

4.1.1 Elevated P450 activity lost in F1 hybrids

The results of the enzymatic assays on adult female mites and teleios confirmed that 18E had a significant 1.80-fold increase in P450 activity compared to the LND negative control in adults and a significant 1.54-fold increase at the teleio stage (Figure

3.6, Table 3.8). It could not be confirmed that P450 activity at the egg stage was increased in 18E, though it is reasonable to conclude that an increase to some degree may be present. The 18E TSSM population showed both a noticeably slow buildup of the I1017F SNP and increased P450 activity, making it reasonable to link these two traits. However, a biological population is not static, and changes occur over time. By the time the genetic crossing experiment took place, the 18E population had lost much of the increased P450 activity and the ♀LND × ♂18E F1 hybrid showed no retention of any increased P450 activity.

4.2 Genetics of I1017F SNP buildup during etoxazole selection

During the course of this investigation a wide range of I1017F SNP build up was observed. All of the greenhouse populations originally collected in Oct. 2018, except for 02E, had I1017F SNP frequencies of 0% during sequencing in Mar. 2020. After the initial 11 months of selection the range of I1017F SNP frequencies observed ranged from 0% - 90%. There were 6 populations (01E, 09E, 10E, 13E, 17E, and 18E) from the original populations plus LNDE that were carried forward for more examination (Figure 4.1). This allowed for additional I1017F SNP frequency data to be collected after 18 months and 31 months of selection.

The TSSM populations undergo maintenance every 7 days, shorter than the time it takes for the mites to reach maturity and oviposit eggs in large numbers (9 days). The rate of turnover of plant material and disposal of mites will shift the mean generation time to a shorter interval. While a small number of adult mites may oviposit eggs over a longer period of time, many mites will only oviposit over a short duration (estimated to be 3 days) before they are removed from the lab kept colonies. A rough estimation of the mean generation time for TSSM populations as they are kept in the lab (see section 2.2) is 10 days, giving the number of generations a month of 3.03. The greenhouse populations were in the lab for 27 months (81.9 generations) in the absence of etoxazole, then on etoxazole selection for an additional 36 months (109.2 generations).

It was hypothesized that the populations that had a noticeably slow rate of buildup of the I1017F SNP may have metabolic resistance to the mild selection pressure used (0.02

mg/L of etoxazole). However, the presence of metabolic resistance was not observed during the experiment, raising the question of alternative explanations for the differential dynamics of the increase in target-site mutation frequency.

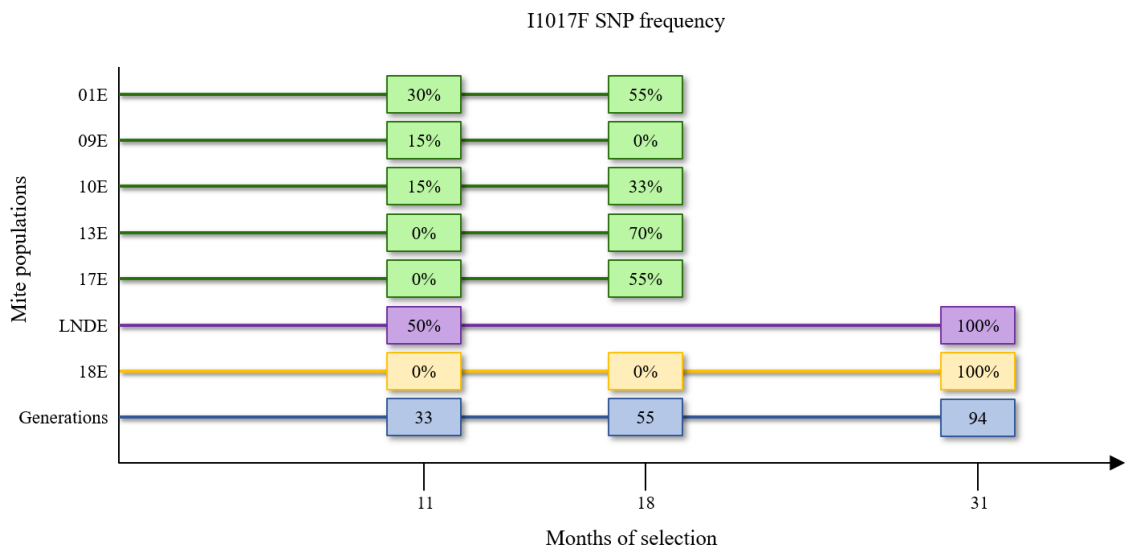


Figure 4.1: I1017F SNP frequency, 11 to 31 months. I1017F SNP frequencies of 6 greenhouse populations put on continuous etoxazole selection at 0.02 mg/L using pretreated leaves over 31 months. All populations had a 0% I1017F SNP frequency at the beginning of etoxazole selection.

4.2.1 Genetic models of recessive allele frequencies

4.2.1.1 Target-site mutation frequency prior to selection

Though the I1017F SNP frequencies have been reported as 0% in this investigation, below a certain threshold the ability to determine the SNP frequency is no longer accurate (see section 2.10.1). Thus, it can be assumed that the I1017F SNP frequency in all the populations put under etoxazole selection was not 0%, as selection was successful in building up the SNP frequency to varying degrees. Figure 4.2 shows a model of 5 hypothetical populations that have low but slightly different frequencies of a recessive allele. The fitness parameters of mites homozygous for a dominant allele, heterozygous, and homozygous for a recessive allele genotypes (AA:Aa:aa) were set to (1.0:1.0:1.1). This scenario reflects a 10% fitness advantage to mites carrying an (aa) genotype, the benefit of

being homozygous for I1017F mutant allele under mild etoxazole selection. The model shows that even a small change in the starting allele frequency can have a dramatic effect on the number of generations it will take for a beneficial recessive allele to become fixed within a population. All populations put on selection with a I1017F SNP frequency reported to be 0%, likely had varying levels of the I1017F SNP at levels below detection. This model shows how the small differences in I1017F SNP frequency can help explain drastically different timelines for the buildup of the target-site mutation.

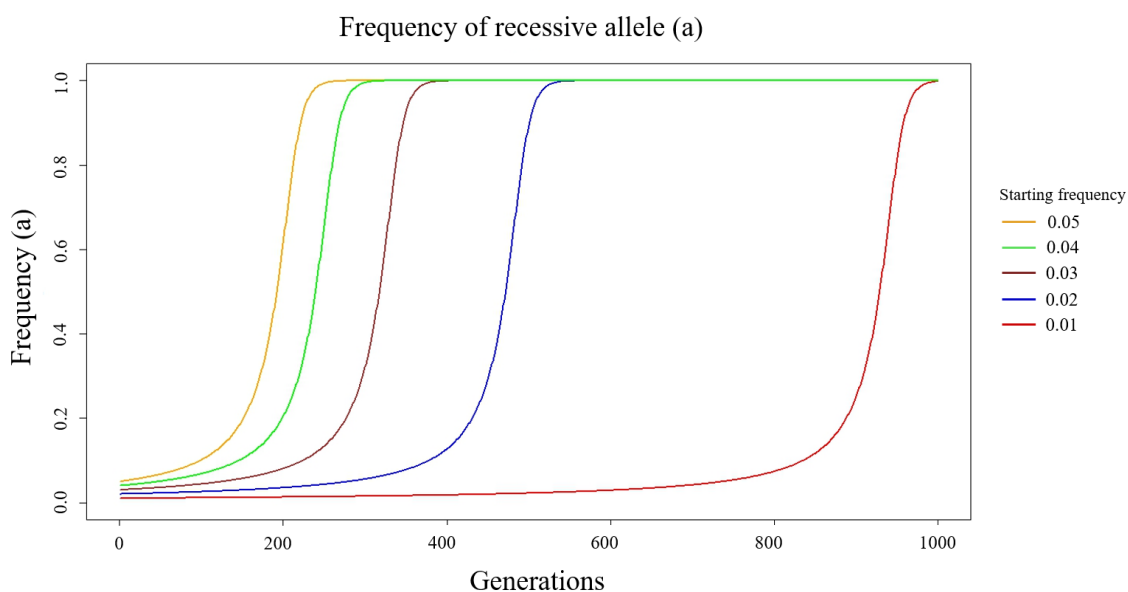


Figure 4.2: Recessive allele frequency model. Model of recessive allele buildup with varying starting allele frequencies of 1% - 5%, fitness parameter (AA:Aa:aa) set to (1.0:1.0:1.1).

4.2.1.2 Effect of mite maintenance on the buildup of the target-site allele

Another potential explanation for the slow buildup of the target-site allele in some populations may be due to mite maintenance. The main lab colony of LND mites is kept on dedicated shelves on intact bean plants spanning multiple plastic trays with a water barrier preventing mites from escaping the colony. This set up allows for the population to be kept in high numbers, estimated to be >10,000. Other mite populations collected for experimentation are kept in the lab as small colonies since space for multiple large colonies

is not available. These additional mite colonies are kept in small containers, as described in section 2.2 and Figure 2.3. Maintenance of these colonies was done every 7 days. Newly stem cut bean plants are placed in the colony and the majority of old material with mites is removed. Typically, a single old stem cut bean plant was carried forward (with occupying mites) with the addition of four fresh plants. This provides enough fresh plant material to feed the colony for the following week while also reducing the population of the colony. Reducing the mite population is necessary, otherwise the mite colony would grow too large for the small container.

In the conditions the colonies are kept, TSSM requires 8 days to reach maturity and 9 days for females to start ovipositing in large numbers. This means that maintenance occurs at a shorter interval than the mites require to mature and oviposit eggs. This results in a large percentage of a colony being composed of individuals that will not have the opportunity to influence the genetics of the colony. As they will not have a chance to mature, mate, and oviposit before they are discarded. For this investigation, the etoxazole selected colonies of LNDE and 18E were kept at a high density to facilitate the removal of 300–400 adult female mites for experimentation. During maintenance it was typical to remove 75% of the plants with occupying TSSM from the colonies to be discarded. The remaining 25% of plant material with approximately 300–700 TSSM individuals were carried forward to continue the colony. A typical population carried forward would have a majority of the individuals being composed of eggs and immature stages. This effectively created a genetic bottleneck effect on the population, one that was repeated every week. Genetic bottlenecks can shift the allele frequency of populations, in a random and unpredictable nature, leading to a genetic drift. Genetic drift can affect allelic frequency due to the random chance of sampling mites that will contribute to the progeny of the next generation. It will influence when or if a recessive allele reaches a high frequency within a population. Figure 4.3 A is a model of the effects of genetic drift on 20 populations each with a starting allele (a) frequency of 50% with no fitness change between genotypes. Figure 4.3 B is a model of genetic drift in 20 populations with a fitness advantage of a homozygous (aa) genotype of 10% and a starting allele frequency of 3%. If the model did not simulate genetic drift, all 20 populations would have identical curves. Genetic drift can have a clear influence on the buildup of the allele frequencies.

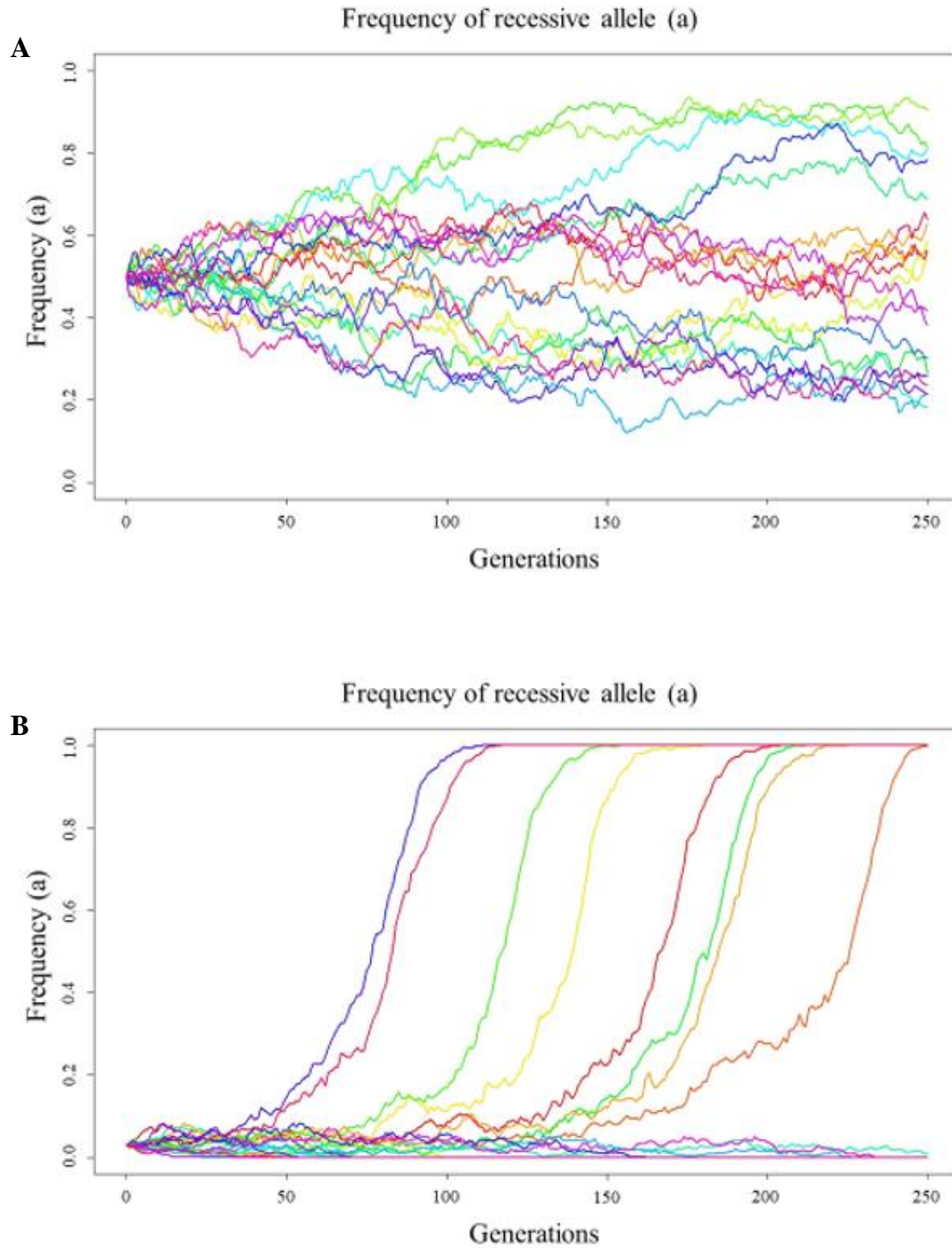


Figure 4.3: Genetic drift recessive allele frequency models. A) genetic drift model with a starting allele (a) frequency of 50%, fitness parameter (AA:Aa:aa) (1.0:1.0:1.0), and effective population of 600. B) genetic drift model with a starting allele (a) frequency of 3%, fitness parameters (AA:Aa:aa) of (1.0:1.0:1.1), effective population of 600.

The genetic bottleneck events occurring during the maintenance of the LNDE and 18E colonies will also intensify inbreeding, another factor that can influence the allelic frequencies in populations. Inbreeding within a population can reduce the frequency of heterozygosity (Figure 4.4).

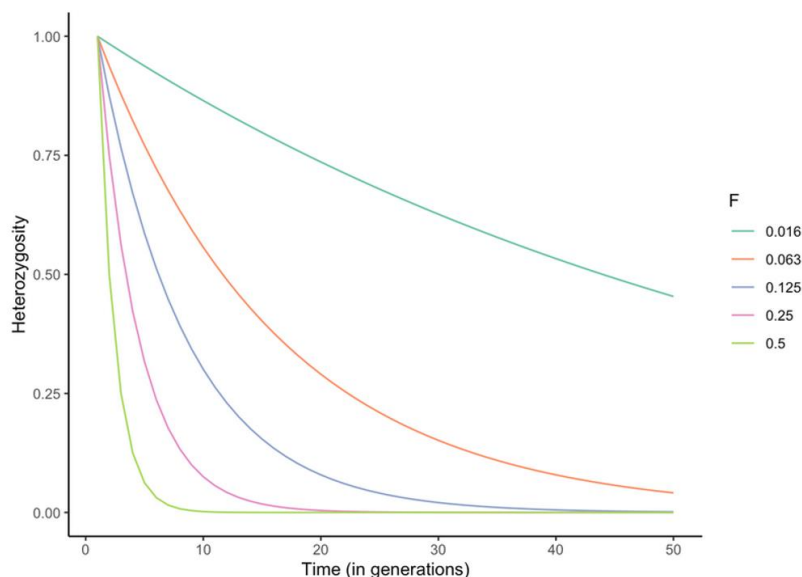


Figure 4.4: Inbreeding effects on heterozygosity. Plot of the influence of inbreeding on the decline of heterozygosity within a population. F = coefficient of inbreeding, $F = 0.5$ self, $F = 0.25$ parent-offspring and full sibling, $F = 0.125$ half siblings, $F = 0.063$ first cousins, and $F = 0.016$ second cousins (Tobler, 2022).

Within the LNDE and 18E colonies the exact biological relationship of mites was not tracked during the genetic bottleneck events occurring in the investigation. Taking into consideration the relative low mobility of females feeding on leaves and their fecundity, some assumptions can be made about the degree of inbreeding after a genetic bottleneck event. TSSM cannot self-fertilize and while parent-offspring fertilization can occur with TSSM, females within these colonies are highly likely to have been fertilized before they began oviposition. Full sibling mating is likely to occur within the LNDE and 18E colonies after a genetic bottleneck, with half sibling, first cousin, and second cousin mating also likely to take place. The degree to which these mating events took place during this investigation cannot be known. It is likely that inbreeding had an effect to decrease the

heterozygosity within the population in both the LNDE and 18E colony. The inbreeding effect may have served to suppress the accumulation of the I1017F SNP when the frequency was low. Conversely, inbreeding may also have increased the accumulation of the I1017F SNP due to etoxazole selection.

4.2.1.3 The effect of haplodiploidy of the buildup of the target-site allele

Previous genetic models were based on diploid species as haplodiploid models of these effects are not readily available. The relationship of expected recessive genotype frequency and corresponding recessive allele frequency within TSSM populations differs between female and male mites (Figure 4.5). TSSM females have an expected genotype (aa) frequency of that of a typical diploid species. Haploid TSSM males will display a genotype (a) at a higher rate, 1:1 with allele frequency. This allows haplodiploid species to fix beneficial autosomal alleles at a higher rate than diploid species (Figure 4.6 A; Dapper et al., 2022). Recessive alleles are also fixed at a higher rate under selection in haplodiploid species than a diploid species (Figure 4.6 B; Bendall et al., 2021).

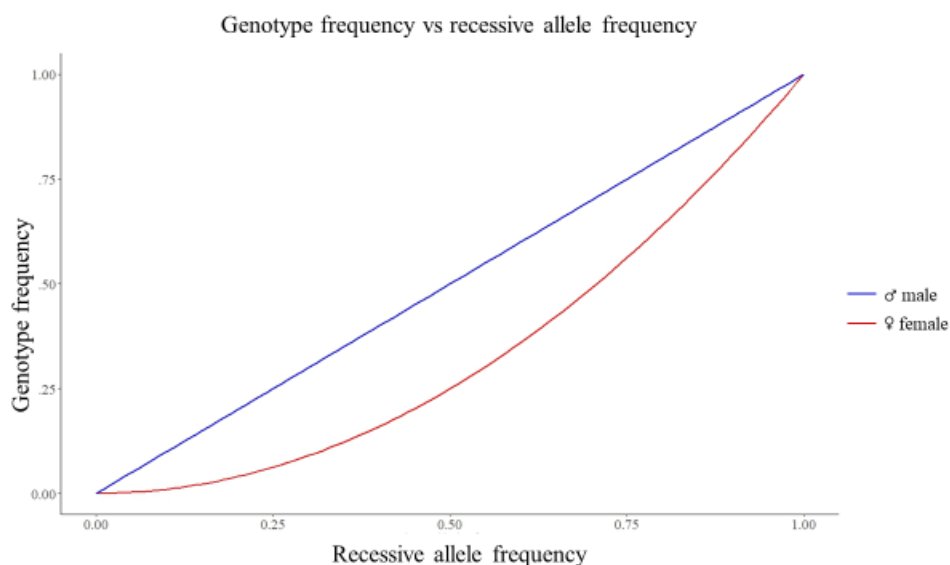


Figure 4.5: Genotype frequency vs recessive allele frequency. Plot of expected genotype frequency of a recessive allele in a TSSM population of diploid female and haploid male

mites. Genotype (aa) frequency = (allele frequency)² for females, genotype (aa) frequency = allele frequency for males.

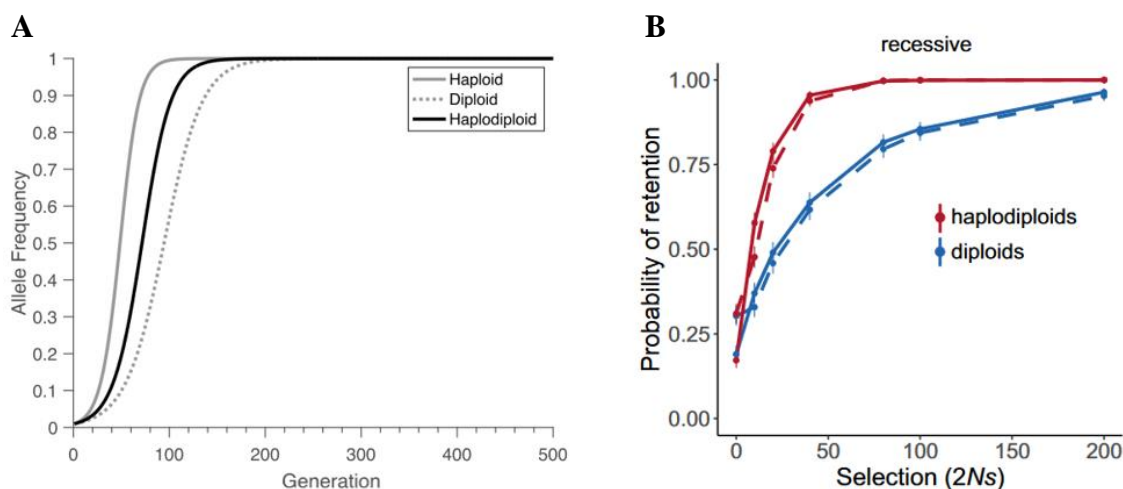


Figure 4.6: Haplodiploid allele fixation. A) Fixation rates over time (generations) of beneficial autosomal alleles in haploid, haplodiploid, and diploid species model (Dapper et al., 2022). B) Retention of recessive alleles plotted against selection pressure for haplodiploid and diploid species (Bendall et al., 2021).

4.2.1.4 Other factors that affect the buildup of the target-site allele

The I1017F SNP is able to confer a high degree of resistance to etoxazole for TSSM but not without a cost. There is an associated fitness penalty to mites carrying two *CHS1* mutant alleles with the I1017F SNP (Bajda et al., 2018). These mites also have longer development times, increased longevity, and greater mean generation times (Bajda et al., 2018). As the I1017F SNP frequency increases, the associated costs will cause shifting dynamics in the fitness parameters within a population.

There may also be other factors that may have influenced the buildup of the target-site mutation within a population. For example, fecundity, male to female ratio, development time, longevity, and gene expression patterns can differ among TSSM populations with different histories of host plants, acaricide exposure, and other factors that can be difficult to track. When these factors are combined with the mild selection pressure of the etoxazole, the unknown level of starting I1017F allele frequency, and the genetic

trends that shift transmission of genetic information to progeny as previously described, it may not be surprising that the TSSM populations displayed a wide temporal variation needed for the fixation of the I1017F allele.

4.3 Metabolic resistance of etoxazole

The detoxification of pesticides by metabolic enzymes is a common resistance strategy used by TSSM, yet evidence that this occurs with etoxazole is not well supported. P450s and CCEs were implicated in a 2017 study in one etoxazole selected population (Adesanya et al., 2017). The exact I1017F SNP frequency of this population was not reported, only that the population had a mix of the wildtype and mutant I1017F *CHSI* alleles. In a 2014 study (Salman & Saritas, 2014) a low level of etoxazole cross resistance in a TSSM population under selection for the pesticide of acequinocyl was associated with elevated CCE activity. No presence of the I1017F allele was reported in the acequinocyl selected population, suggesting that the resistance to etoxazole was due to the activity of CCEs. In the predatory mite, *Phytoseiulus persimilis*, a study of an etoxazole selected population implicated P450s, CCEs, and GSTs in etoxazole resistance (Salman et al., 2015). However, direct evidence of metabolic resistance to etoxazole is limited.

Examining cross resistance in etoxazole selected populations has also raised the possibility of involvement of detoxifying metabolic enzymes, specifically P450s, interacting with etoxazole. A 2021 study, (Koo et al., 2021), examined acaricide cross resistance in an etoxazole selected TSSM population. The highly etoxazole resistant TSSM population showed cross resistance to abamectin at the egg stage (RR=10.6), though not in adults, and resistance to pyflubumide in eggs (RR=682.8) and adults (RR>727.3) (Koo et al., 2021). Abamectin and pyflubumide do not share a target-site with etoxazole. The targets of abamectin are GABA gated chloride channels (GABA_{Cl}) and glutamate-gated chloride channels (GluCl), while the target of pyflubumide is mitochondrial complex II (Clark et al., 1995; Wolstenholme, 2010; Nakano et al., 2015). Interestingly, P450s have been linked to both abamectin and pyflubumide resistance (Riga et al., 2014; Fotoukkaia et al., 2020). However, the majority of studies of etoxazole resistance in TSSM do not find evidence of metabolic resistance. Similar to this investigation, etoxazole resistance appears to be dependent on the presence of the recessive I1017F *CHSI* allele. It is possible that

metabolic resistance to etoxazole does not occur in TSSM, though two hypothetical scenarios will be proposed in an attempt to reason why metabolic resistance may be possible but difficult to isolate.

4.3.1 Scenario 1: TSSM embryo (egg) bottleneck

The inhibition of CHS1 activity by etoxazole is fatal to the TSSM at the egg, larvae, and nymph stage (Dekeyser, 2005). The Van Leeuwen et al. (2012) study did not show a reduction in fecundity of treated adult female TSSM but did show a high mortality in the eggs the treated females oviposited, reducing fertility of adult female mites. An individual homozygous for the I1017F *CHS1* allele will have an extreme resistance to etoxazole at all stages of development, which may not be the case for metabolic resistance.

As a TSSM progresses through development, the gene expression changes. This could also include the expression of enzymes involved in metabolic resistance. Gene expression data for P450s, CCEs, and GSTs, confirm that the expression pattern of these genes vary at the embryo (egg), larval, nymph, and adult stage (Figure 4.7, Grbic et al. 2011). Of the 89 P450, 72 CCE, and 33 GST genes, there are genes expressed at high and low levels common in all stages, though there are differences. Compared to the other stages of development the embryo stage has noticeably lower expression for many genes of these 3 enzymes classes. If genes that are at a lower expression level in embryos do contribute to etoxazole resistance, then embryos have a reduced ability to metabolize pesticides relative to other development stages.

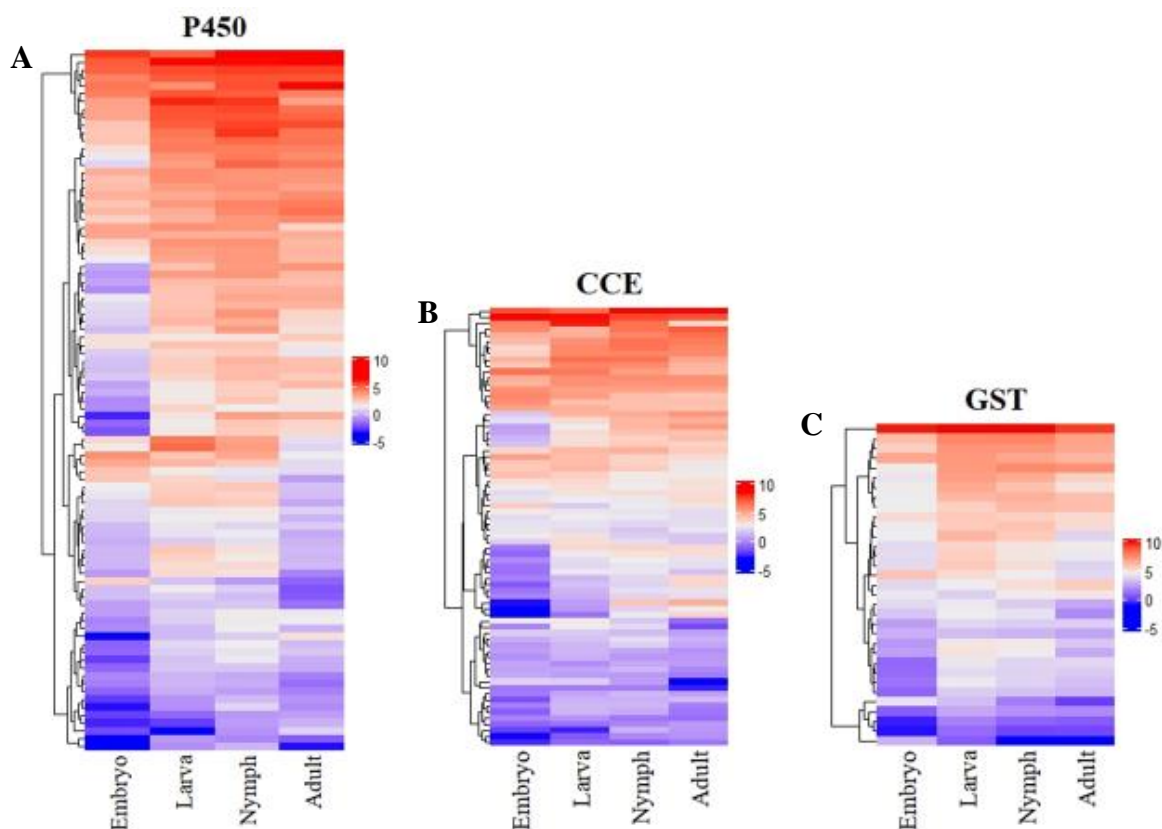


Figure 4.7: Gene expression heatmaps by development stage. A) Cytochrome P450 gene expression heatmap, 89 P450 genes. B) Carboxyl/cholinesterases gene expression heatmap, 72 CCE genes. C) Glutathione-S-transferases gene expression heatmap, 33 GST genes. All heatmaps use euclidean distance of \log^2 FPKM data and hierarchical clustering at 4 stages of development. Data obtained from Gene Expression Omnibus series GSE31527 (Grbic et al., 2011) courtesy of Vladimir Zhurov.

In the hypothetical case an individual TSSM can survive exposure to an acaricide at the larval, nymph, or adult stage due to a detoxifying enzyme activity, potential offspring at the egg stage may still be vulnerable to the acaricide due to decreased gene expression of genes encoding detoxifying enzymes. In such a scenario, the metabolic enzyme activity that enables a parent mite to survive may not be present in the offspring at the egg stage, resulting in mortality of the offspring. Thus, the embryo stage may represent a barrier for the inheritance of increased enzymatic activity in this scenario.

4.3.2 Scenario 2: Target-site mutation suppression of selection pressure

During the course of this investigation at a certain point in time (July 2021), population 09E and 18E had continued to gain etoxazole resistance with no corresponding increase in I1017F SNP frequency. The resulting sampling of adult and teleios of 18E in December 2021 revealed elevated P450 activity in 18E that was a potential explanation of the increased resistance for this population. However, later data revealed that this increased P450 activity is transient and was largely lost by the time the populations were sampled during the genetic crossing experiment. The evidence found in literature that supports metabolic resistance in TSSM to etoxazole was either in a population with I1017F below 100% (Adesanya et al., 2017) or a population with no reported presence of I1017F (Salman & Saritas, 2015).

In theory, any target-site mutation (I1017F) or metabolic resistance that increases mite fitness will be selected for etoxazole selection. The continued presence of etoxazole selection pressure should result in increased frequency of the I1017F SNP and metabolic detoxifying activity. The I1017F SNP has been linked to a fitness cost in TSSM and increased P450 activity has been shown to have a negative impact on fitness and fertility in *Anopheles funestus*, the African malaria mosquito (Stocco et al., 2016; Badja et al., 2018; Tchouakui et al., 2020). Given the extreme protection to etoxazole provided by the I1017F allele (homozygous mite are functionally immune to etoxazole), the etoxazole selection pressure ceases to exist. Thus, if an increased metabolic enzyme activity was selected for prior to I1017F SNP frequency reaching 100%, once the I1017F SNP is fixed the metabolic activity is expected to be lost over time due to a fitness cost (Figure 4.8).

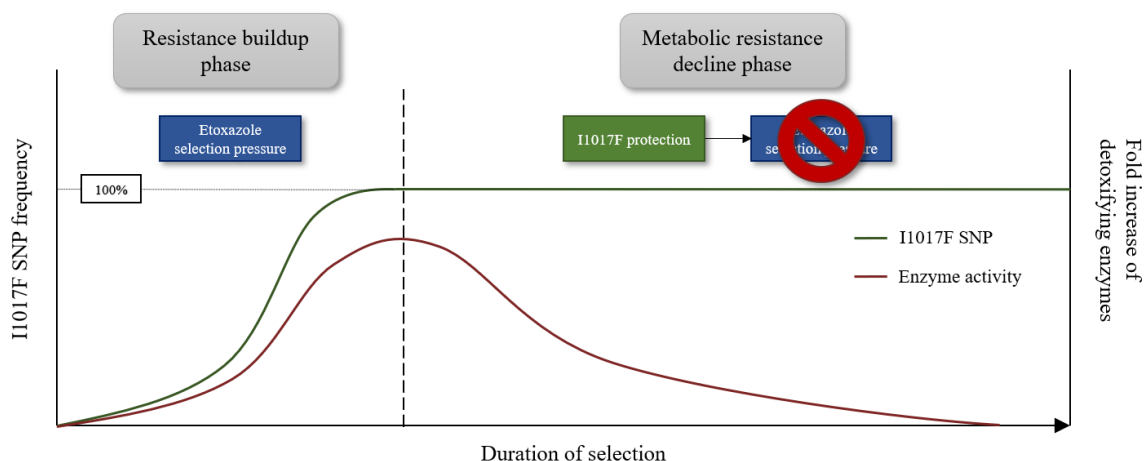


Figure 4.8: Target-site suppression of selection pressure model. Model of the theorized relationship between I1017F SNP frequency and metabolic resistance as I1017F is fixed at 100%.

The interplay between target-site mutations and metabolic enzymes in relationship to pesticide resistance has been shown to be beneficial in some cases. In *Drosophila melanogaster*, the common fruit fly, resistance to a pyrethroid pesticide by target-site mutation and increased P450 activity was found to have a synergistic relationship (Samantsidis et al., 2020). The combined effect of a target-site mutation and increased P450 activity worked together to provide a higher degree of protection than either resistance mechanism was able to provide alone, though the combination also carried an increased fitness cost (Samantsidis et al., 2020). However, in this case and unlike the situation in mites' resistance to etoxazole, the target-site mutation does not lead to complete insensitivity to the pesticide. Homozygosity for I1017F *CHS1* alleles is sufficient to protect mites against etoxazole, while any potential protection from increased P450 activity could occur in mites carrying one or more wildtype *CHS1* alleles.

4.4 I1017F SNP cross resistance

The focus of this study was on etoxazole resistance within TSSM populations. However, it is worth noting that the I1017F SNP within *CHS1* provides TSSM with protection to benzoylurea insecticides and multiple acaricides of the mite growth inhibitor class, including etoxazole, clofentezine, and hexythiazox (Demaeght et al., 2014; Douris

et al., 2016; Riga et al., 2017). The effects of a target-site mutation on these other pesticides are currently not known.

5 Summary & Conclusion

Etoxazole is a potent acaricide capable of causing mortality and molting defects in eggs, larvae, and nymphs of TSSM and causing infertility in adults. A recessive mutation in the target-site of *CHSI* (I1017F) provides a high level of resistance if an individual is homozygous for the mutant allele. There is limited evidence for the possibility of metabolic resistance to etoxazole in TSSM. During the course of this investigation a delay in the buildup of the I1017F SNP and continued buildup of resistance in TSSM populations under selection pressure from etoxazole at 0.02 mg/L was observed. Further investigation revealed that one of the TSSM populations (18E) also had increased activity of P450s, a common enzyme class involved in detoxifying xenobiotics. A genetic crossing protocol was used in order to create F1 hybrids heterozygous for *CHSI* alleles (wildtype and I1017F mutant) and therefore lacking the target-site resistance to etoxazole the recessive I1017F mutant allele provides. The F1 hybrids displayed a susceptible phenotype to etoxazole with a small shift toward resistance when compared to the LND susceptible control. No increased P450 activity was found in the F1 hybrids. The shift in resistance was attributed to an unexpected presence of the I1017F mutant allele in the LND mite population, creating a small occurrence of F1 hybrids homozygous for the I1017F mutant allele.

The presence of metabolic resistance could not be found within the greenhouse mite populations collected from commercial greenhouses in Ontario. The resistance to etoxazole observed throughout the investigation could only be linked to the presence of the I1017F mutation in *CHSI*. This mutation is capable of providing an extreme tolerance to etoxazole in individual TSSM homozygous for the I1017F mutant allele, making the mite functionally immune to etoxazole. A loss of a single I1017F mutant allele in subsequent generations can restore the etoxazole susceptible phenotype. While the possibility of metabolic resistance to etoxazole in TSSM cannot be ruled out, the I101F SNP is the dominant source of etoxazole resistance both in field collected and lab TSSM populations.

6 Future directions

The ability of TSSM to resist etoxazole by the I1017F mutant allele is well established, yet there remains a question of whether the TSSM is capable of metabolic resistance to etoxazole. Mortality in eggs due to etoxazole was the focus of this investigation and is a common development stage for the study of etoxazole resistance, though all immature stages are vulnerable to mortality by etoxazole. Further study into the dynamics of etoxazole resistance in a TSSM population of all development stages, the population dynamic commercial growers deal with, may reveal nuances of how TSSM populations are able to adapt to etoxazole. This may also give insight on the hypothesized effect termed “Embryo (egg) bottleneck”, should metabolic resistance be observed in any development stage.

Investigation into etoxazole resistance, and pesticide resistance in general, is hampered by the shifting nature of TSSM resistance status. The TSSM’s ability to adapt can shift resistance during the course of an investigation. A comprehensive and rigidly timed observation of how the resistance to etoxazole shifts over time within a population, the corresponding change in I1017F, and any change in detoxifying enzyme activity in all development stages would be informative. This would be very challenging, ideally all development stages and trials would be in the same generation, requiring a large mite population that could withstand the sampling.

A closer examination of cross resistance to etoxazole in TSSM populations with no history of the I1017F mutant allele may be worthwhile. It may seem counterintuitive, but the high degree of protection the I1017F allele gives can easily obscure any evidence of metabolic resistance. As previously mentioned, the evidence found in literature that supports metabolic resistance in TSSM from (Adesanya et al., 2017) and (Salman & Saritas, 2015) was from mite populations with an I1017F SNP below 100% or with no reported presence of I1017F. A study of etoxazole selection in a predatory mite, *Phytoseiulus persimilis*, which does not possess an I1017F mutation in the species also supports the prospect of metabolic resistance to etoxazole (Salman et al., 2015). However, relying on TSSM populations collected in the field to find populations lacking the I1017F

allele may prove difficult, all original populations collected from commercial greenhouses that were part of this investigation had I1017F SNP frequencies of 100% during initial genotyping.

The practical applications of the dominance of the recessive I1017F allele in etoxazole resistance in TSSM may prove beneficial in some regards. The I1017F SNP would be an ideal genetic marker for commercial growers to indicate whether etoxazole would be an effective control measure, due to the high degree of etoxazole resistance the I1017F SNP confers when both *CHSI* alleles have the mutation. TSSM populations with the I1017F SNP would either be largely resistant to etoxazole or capable of rapidly building resistance. This would eliminate etoxazole as a possible control method for the commercial grower.

In the situation that a population had a high frequency of the I1017F SNP and limited available treatment options, the recessive nature of the I1017F and general lack of metabolic resistance observed could be exploited. If a large number of male mites with a wildtype *CHSI* allele were introduced into a highly resistant population currently infesting a field, it may quickly render a large portion of the population susceptible to etoxazole. The generation of a large number of males is not a difficult task. During this investigation, populations of almost exclusively males in numbers of approximately 2000 – 3000 combined were generated by one person with 2 – 3 hours' time infesting leaves with teleios. This method could produce a large number of males if scaled up with more personnel and time for infestation. This method would require a time of 9 – 10 days to prepare the males for introduction into a resistant population. Any females already fertilized in a highly resistant population would continue to produce resistant offspring, as the genetics of offspring is largely unchanged with additional mating after the first mating event (Potter & Wrensch, 1978). However, the susceptible males will fertilize any newly emerged females. If the ratio of susceptible males to resistant males already in the population is high, the population may shift in resistance status to a significant degree in as little as a single generation. This strategy would need to be investigated to determine if it may be a viable solution to growers with little or no viable options in pesticide selection.

References

- Adesanya, A. W., Morales, M., Walsh, D. B., Lavine, L. C., Lavine, M. D., & Zhu, F. 2018. Mechanisms of resistance to three mite growth inhibitors of *Tetranychus urticae* in hops. *Bulletin of Entomological Research*, 108(1), 23–34. <https://doi.org/10.1017/S0007485317000414>
- Arena, M., Auteri, D., Barmaz, S., Bellisai, G., Brancato, A., Brocca, D., Bura, L., Byers, H., Chiusolo, A., Court Marques, D., Crivellente, F., De Lentdecker, C., De Maglie, M., Egsmose, M., Erdos, Z., Fait, G., Ferreira, L., Goumenou, M., Greco, L., Ippolito, A., Istace, F., Janossy, J., Jarrah, S., Kardassi, D., Leuschner, R., Lythgo, C., Magrans, J. O., Medina, P., Miron, I., Molnar, T., Nougadere, A., Padovani, L., Morte, J. M. P., Pedersen, R., Reich, H., Sacchi, A., Santos, M., Serafimova, R., Sharp, R., Stanek, A., Streissl, F., Sturma, J., Szentcs, C., Tarazona, J., Terron, A., Theobald, A., Vagenende, B., Verani, A., & Villamar-Bouza, L. (2017). Peer review of the pesticide risk assessment of the active substance etoxazole. *EFSA Journal*, 15(10), e04988–e04988. <https://doi.org/10.2903/j.efsa.2017.4988>
- Bajda, S., Riga, M., Wybouw, N., Papadaki, S., Ouranou, E., Fotoukiki, S. M., Vontas, J., Van Leeuwen, T. 2018. Fitness costs of key point mutations that underlie acaricide target-site resistance in the two-spotted spider mite *Tetranychus urticae*. *Evolutionary Applications*, 11(9), 1540–1553. <https://doi.org/10.1111/eva.12643>
- Bendall, E. E., Bagley, R. K., Sousa, V. C., Linnen, C R. 2022. Faster-haplodiploid evolution under divergence-with-gene-flow: Simulations and empirical data from pine-feeding hymenopterans. *Molecular ecology*. [Online] 31 (8), 2348–2366.
- Bensoussan, N., Santamaria, M. E., Zhurov, V., Diaz, I., Grbic, M., & Grbic, V. (2016). Plant-herbivore interaction: dissection of the cellular pattern of *Tetranychus urticae* Feeding on the Host Plant. *Frontiers in Plant Science*, 7, Article 1105. <https://doi.org/10.3389/fpls.2016.01105>
- Bradford, M. M. 1976. A rapid and sensitive method for the quantitation of microgram quantities of protein utilizing the principle of protein-dye binding. *Analytical Biochemistry*, 72(1), 248–254. [https://doi.org/10.1016/0003-2697\(76\)90527-3](https://doi.org/10.1016/0003-2697(76)90527-3)

- Clark, J. K., Scott, J. G., Campos, F., & Bloomquist, J. R. 1995. Resistance to avermectins: extent, mechanisms, and management implications. *Annual Review of Entomology*, 40(1), 1–30. <https://doi.org/10.1146/annurev.en.40.010195.000245>
- Dapper, Slater, G. P., Shores, K., & Harpur, B. A. (2022). Population Genetics of Reproductive Genes in Haplodiploid Species. *Genome Biology and Evolution*, 14(6). <https://doi.org/10.1093/gbe/evac070>
- Dekeyser M.A. 2005. Acaricide mode of action. *Pest Manag. Sci.*, v.61, pp.103.
- Demaeght, P., Osborne, E. J., Odman-Naresh, J., Grbić, M., Nauen, R., Merzendorfer, H., Clark, R. M., & Van Leeuwen, T. 2014. High resolution genetic mapping uncovers chitin synthase-1 as the target-site of the structurally diverse mite growth inhibitors clofentezine, hexythiazox and etoxazole in *Tetranychus urticae*. *Insect Biochemistry and Molecular Biology*, 51, 52–61. <https://doi.org/10.1016/j.ibmb.2014.05.004>
- Dermauw, W., Wybouw, N., Rombauts, S., Menten, R., Vontas, J., Grbic, M., Clark, R.M., Feyereisen, R., Van Leeuwen, T. 2013. Link between host plant adaptation and pesticide resistance in the polyphagous spider mite *Tetranychus urticae*. *Proc. Natl. Acad. Sci. U S A* 100, E113eE122.
- Douris, V., Steinbach, D., Panteleri, R., Livadaras, I., Pickett, J. A., Van Leeuwen, T., Nauen, R., & Vontas, J. (2016). Resistance mutation conserved between insects and mites unravels the benzoylurea insecticide mode of action on chitin biosynthesis. *Proceedings of the National Academy of Sciences - PNAS*, 113(51), 14692–14697. <https://doi.org/10.1073/pnas.1618258113>
- Feyereisen, R., 2005. Insect cytochrome P450. In: Gilbert, L.I., Iatrou, K., Gill, S. (Eds.), *Comprehensive insect physiology, biochemistry, pharmacology and molecular biology*. Elsevier, Amsterdam, pp. 1e77.
- Feyereisen, R., 2006. Evolution of insect P450. *Biochem. Soc. Trans.* 34, 1252e1255.

- Feyereisen, R., Dermauw, W., & Van Leeuwen, T. 2015. Genotype to phenotype, the molecular and physiological dimensions of resistance in arthropods. *Pesticide Biochemistry and Physiology*, 121, 61–77. <https://doi.org/10.1016/j.pestbp.2015.01.004>
- Fotoukkaiai, S. M., Mermans, C., Wybouw, N., & Van Leeuwen, T. 2020. Resistance risk assessment of the novel complex II inhibitor pyflubumide in the polyphagous pest *Tetranychus urticae*. *Journal of Pest Science*, 93(3), 1085–1096. <https://doi.org/10.1007/s10340-020-01213-x>
- Grbic, M., Van Leeuwen, T., Clark, R. M., Rombauts, S., Rouze, P., Grbic, V., Osborne, E. J., Dermauw, W., Thi Ngoc, P. C., Ortego, F., Hernandez-Crespo, P., Diaz, I., Martinez, M., Navajas, M., Sucena, E., Magalhaes, S., Nagy, L., Pace, R. M., Djuranovic, S., Smagghe, G., ... Van de Peer, Y. 2011. The genome of *Tetranychus urticae* reveals herbivorous pest adaptations. *Nature* 479, 487–492. <https://doi.org/10.1038/nature10640>
- Hebert, H. J. 1981. (Acarina: Tetranychidae). *Can. Entomol.*, 113, pp. 371-378.
- Kennedy, C., & Tierney, K. 2013. Xenobiotic protection/resistance mechanisms in organisms. In *Environmental Toxicology: Selected Entries from the Encyclopedia of Sustainability Science and Technology*, ed. EA Laws, pp. 689–721. New York: Springer.
- Koo, H-N., Choi, J., Shin, E., Kang, W., Cho, S.-R., Kim, H., Park, B., & Kim, G.-H. 2021. Susceptibility to acaricides and the frequencies of point mutations in etoxazole- and pyridaben-resistant strains and field populations of the two-spotted spider mite, *Tetranychus urticae* (acari: tetranychidae). *Insects (Basel, Switzerland)*, 12(7), 660–. <https://doi.org/10.3390/insects12070660>
- Kwon, D. H., Lee, S. W., Ahn, J. J., & Lee, S. H. 2014. Determination of acaricide resistance allele frequencies in field populations of *Tetranychus urticae* using quantitative sequencing. *Journal of Asia-Pacific Entomology*, 17(1), 99–103. <https://doi.org/10.1016/j.aspen.2013.11.001>

- Liburd, O.E., & Finn, E.M. 2004. Small fruit pests and their management. *In Encyclopedia of Entomology*. Springer, Dordrecht. https://doi-org.proxy1.lib.uwo.ca/10.1007/0-306-48380-7_3943
- Migeon, A., & Dorkeld, F. 2006–2023. Spider mites web: a comprehensive database for the tetranychidae. Available online at: <http://www.montpellier.inra.fr/CBGP/spmweb> (Accessed on December 13, 2020).
- Merzendorfer. 2006. Insect chitin synthases: a review. *Journal of Comparative Physiology. B, Biochemical, Systemic, and Environmental Physiology*, 176(1), 1–15. <https://doi.org/10.1007/s00360-005-0005-3>
- Merzendorfer, H. 2013. Chitin synthesis inhibitors: old molecules and new developments. *Insect Science*, 20: pp. 121-138.
- Nakano, M., Yasokawa, N., Suwa, A., Fujioka, S., Furuya, T., & Sakata, K. 2015. Mode of action of novel acaricide pyflubumide: Effects on the mitochondrial respiratory chain. *Journal of Pesticide Science*, 40(1), 19–24. <https://doi.org/10.1584/jpestics.D14-086>
- Oliver, J. H. 1971. Parthenogenesis in mites and ticks (Arachnida-Acari) *Am. Zool.*, 11, pp. 283-299.
- Potter, D. A. & Wrensch, D. L. 1978. Interrupted matings and the effectiveness of second inseminations in the twospotted spider mite. *Annals of the Entomological Society of America*, 71(6), 882–885. <https://doi.org/10.1093/aesa/71.6.882>
- Riga, M., Tsakireli, D., Ilias, A., Morou, E., Myridakis, A., Stephanou, E. G., Nauen, R., Dermauw, W., Van Leeuwen, T., Paine, M., & Vontas, J. 2014. Abamectin is metabolized by CYP392A16, a cytochrome P450 associated with high levels of acaricide resistance in *Tetranychus urticae*. *Insect Biochemistry and Molecular Biology*, 46, 43–53. <https://doi.org/10.1016/j.ibmb.2014.01.006>
- Riga, M., Bajda, S., Themistokleous, C., Papadaki, S., Palzewicz, M., Dermauw, W., Vontas, J., & Leeuwen, T. V. 2017. The relative contribution of target-site mutations in complex acaricide resistant phenotypes as assessed by marker assisted

- backcrossing in *Tetranychus urticae*. *Scientific Reports*, 7(1), 9202–9212. <https://doi.org/10.1038/s41598-017-09054-y>
- Ritz, Baty, F., Streibig, J. C., & Gerhard, D. 2015. Dose-response analysis using R. *PLoS One*, 10(12), e0146021–e0146021. <https://doi.org/10.1371/journal.pone.0146021>
- Salman, Y. S., Aydinlt, A., Ay, R. 2015. Etoxazole resistance in predatory mite *Phytoseiulus persimilis* A.-H. (Acari: Phytoseiidae): Cross-resistance, inheritance, and biochemical resistance mechanisms. *Pesticide biochemistry and physiology*. [Online] 12296–102.
- Salman, Y. S., & Saritaş, E. 2014. Acequinocyl resistance in *Tetranychus urticae* koch (acari: tetranychidae): inheritance, synergists, cross-resistance and biochemical resistance mechanisms. *International Journal of Acarology*, 40(6), 428–435. <https://doi.org/10.1080/01647954.2014.944932>
- Samantsidis, G-R., Panteleri, R., Denecke, S., Kounadi, S., Christou, I., Nauen, R., Douris, V., & Vontas, J. 2020. “What I cannot create, I do not understand”: functionally validated synergism of metabolic and target-site insecticide resistance. *Proceedings of the Royal Society. B, Biological Sciences*, 287(1927), 20200838–. <https://doi.org/10.1098/rspb.2020.0838>
- Sparks, T. C., & Nauen, R. 2015. IRAC: mode of action classification and insecticide resistance management. *Pesticide Biochemistry and Physiology*, 121, 122–128. <https://doi.org/10.1016/j.pestbp.2014.11.014>
- Staden, R. 1996. Staden sequence analysis package. *Molecular Biotechnology*, 5(3), 233–241. <https://doi.org/10.1007/BF02900361>
- Stocco, R. S. M., Sato, M. E., & Santos, T. L. 2016. Stability and fitness costs associated with etoxazole resistance in *Tetranychus urticae* (Acari: Tetranychidae). *Experimental & Applied Acarology*, 69(4), 413–425. <https://doi.org/10.1007/s10493-016-0054-1>
- Stumpf, N., & Nauen, R. 2001. Cross-resistance, inheritance, and biochemistry of mitochondrial electron transport inhibitor-acaricide resistance in *Tetranychus*

- urticae* (acari: tetranychidae). *Journal of Economic Entomology*, 94(6), 1577–1583.
<https://doi.org/10.1603/0022-0493-94.6.1577>
- Tchouakui, M., Riveron Miranda, J., Mugenzi, L. M. J., Djonabaye, D., Wondji, M. J., Tchoupo, M., Tchapga, W., Njiokou, F., & Wondji, C. S. 2020. Cytochrome P450 metabolic resistance (CYP6P9a) to pyrethroids imposes a fitness cost in the major African malaria vector *Anopheles funestus*. *Heredity*, 124(5), 621–632.
<https://doi.org/10.1038/s41437-020-0304-1>
- Tobler, M. 2022. A primer of evolution: an introduction to evolutionary thought: theory, evidence, and practice. <https://www.k-state.edu/biology/p2e/evolutionary-mechanisms-ii-mutation-genetic-drift-migration-and-non-random-mating.html>.
- Tuan, S.-J., Lin, Y.-H., Yang, C.-M., Atlihan, R., Saska, P., & Chi, H. 2016. Survival and reproductive strategies in two-spotted spider mites: demographic analysis of arrhenotokous parthenogenesis of *Tetranychus urticae* (acari: tetranychidae). *Journal of Economic Entomology*, 109(2), 502–509.
<https://doi.org/10.1093/jee/tov386>
- Valent. 2015. TetraSan™ 5 WDG miticide: directions for use on greenhouse tomatoes. Retrieved from:
https://www.plantproducts.com/ca/images/TetraSan_Miticide_label_2015-10-30.pdf
- Van Leeuwen, Demaeght, P., Osborne, E. J., Dermauw, W., Gohlke, S., Nauen, R., Grbić, M., Tirry, L., Merzendorfer, H., & Clark, R. M. 2012. Population bulk segregant mapping uncovers resistance mutations and the mode of action of a chitin synthesis inhibitor in arthropods. *Proceedings of the National Academy of Sciences - PNAS*, 109(12), 4407–4412. <https://doi.org/10.1073/pnas.1200068109>
- Van Leeuwen, T., & Dermauw, W. 2016. The molecular evolution of xenobiotic metabolism and resistance in chelicerate mites. *Annual Review of Entomology*, 61(1), 475–498. <https://doi.org/10.1146/annurev-ento-010715-023907>
- Van Leeuwen, T., Vontas, J., Tsagkarakou, A., & Tirry, L. 2009. Mechanisms of acaricide resistance in the two-spotted spider mite *Tetranychus urticae*. In *Biorational*

Control of Arthropod Pests (pp. 347–393). Springer Netherlands.
https://doi.org/10.1007/978-90-481-2316-2_14

Wolstenholme, A. J. 2010. Recent progress in understanding the interaction between avermectins and ligand-gated ion channels: putting the pests to sleep. *Invertebrate Neuroscience*, 10(1), 5–10. <https://doi.org/10.1007/s10158-010-0105-y>

Zhao, X., Gou, X., Qin, Z., Li, D., Wang, Y., Ma, E., Li, S., & Zhang, J. 2017. Identification and expression of cuticular protein genes based on *Locusta migratoria* transcriptome. *Scientific Reports*, 7(1), 45462–45462. <https://doi.org/10.1038/srep45462>

Appendices

Appendix A: Software used during investigation.

Table A1: Software Information.

Information	Entry
R	
version	R version 4.2.2 (2022-10-31)
os	Windows 11 22H2 22621.1413
system	x86_64-w64-mingw32/x64
R studio	
version	2022.07.1 Build 554
packages	tidyr
	dplyr
	gplots
	ggplot2
additional packages for dose response analysis	
	drc
additional packages for genetic models	
	learnPopGen
additional packages for heatmaps	
	ComplexHeatmap

Curriculum Vitae

Name: Jeremy Spenler

Post-secondary Education and Degrees: University of Waterloo
Waterloo, Ontario, Canada
2008-2014 B.Sc.

The University of Western Ontario
London, Ontario, Canada
2020-2023 M.Sc.

Related Work Experience

Laboratory Technician
The University of Western Ontario
2019-2020

Teaching Assistant
London, Ontario, Canada
2021